Mathematics in Art:
An Exhibition at the Singapore Art Museum

Siu Mee Lin

An academic exercise presented in partial fulfillment for the degree of Bachelor of Science with Honours in Mathematics.

Supervisor : A/P Helmer Aslaksen

Department of Mathematics
National University of Singapore
2001/2002

Acknowledgements

I would like to express my gratitude to my Supervisor, A/P Helmer Aslaken, for his patience, guidance and encouragement throughout the process of doing this project. He has been very helpful and has given invaluable advice to improve myself along the way.

I would also like to thank the following people: my family for understanding the little time I had spent with them; my hallmates Johnny and Eryan for their encouragement and understanding; my pal Bernard for the numerous discussions on my project; my seniors Kim Yong and Sean Chung for their advice and support; Chin Ann for his time; Shin Yeow for always being there and to proof-read my thesis.

Summary

This thesis serves as an introductory text for readers to understand the relation between Art and Mathematics. It aims to provide an insight to the readers how attractive figures can be analyzed mathematically and how we are surrounded by Art and Mathematics everyday.

Chapter 1 arms the readers with some knowledge of symmetry. With that, readers will learn how patterns can be classified according to the symmetries they admit. Chapter 2 touches the topic of tilings. As the topic of tilings is quite a big one, only tilings by regular polygons are discussed. In Chapter 3, we explore the world of fractals. Keeping in mind this thesis is an introductory account in nature, I try not to go into too much technicalities. In fact, I try to keep the chapter as interesting and simple as possible. Chapter 4 on kaleidoscopes is a chapter that allows the readers to have some hands on experience with mirrors to create some attractive figures. Finally, Chapter 5 discusses two controversial issues about the golden ratio. One issue is whether the golden ratio is present in the ancient architectural construction of the Parthenon. The other one is whether the rectangle that embodies the golden ratio is the most aesthetically pleasing rectangle.

Author's Contributions

I have done the following in this project:

1) Revision of the flow chart for wallpaper symmetry groups presented by Washburn and Crowe **[1]**. My revised flow chart is found on page 22.

2) Using *Kaleidomania!*™ to generate Figure 1.3.1b, Figure 1.3.3 and the figures in Tables 1.2.1, 1.4.1, 1.5.1, 1.6.1 and 1.6.2.

3) Analysis and classification of edge-to-edge tilings by regular polygons into their symmetry groups, which is presented in Table 2.3.1 from pages 36 to 38.

4) Deriving the iterated function systems (IFS) of the symmetric fractals presented in Table 3.6.1 on pages 47 and 48 and generating the symmetric fractals using the software *Fractal Explorer*. The details of deriving the IFS are found in Appendix I, pages 68 to 71.

5) Checking if golden rectangles are the most aesthetically pleasing rectangle by conducting a survey. The survey form and the results are found in Appendix II, pages 72 and 73. From the results of my survey, I concluded that golden rectangles are not necessarily the most aesthetically appealing rectangles.

CONTENTS

Chapter 1

Symmetry Groups

1.1 Introduction

In this chapter, we are interested in the underlying structure of aesthetically pleasing plane figures. By a *plane figure*, we mean any subset of the plane. To understand the underlying structure, we examine the symmetries of the figure. An *isometry* of the plane is a distance-preserving transformation of the plane. This means that for any pair of points P and Q, the distance between the images under the transformation is the same as the distance between P and Q. A *symmetry* of a figure is an isometry that maps the figure back onto itself. There are four types of isometries, namely translation, reflection, rotation and glide reflection. A short description of each isometry of the plane is given in the next section. We will classify a figure in terms of its *symmetry group*, which is the set of all symmetries of the figure. If a figure admits a symmetry, it is said to be *symmetrical*.

We will first give a brief description of the four types of isometries of the plane after which we will show how to recognise the symmetry group of a figure.

1.2 The Four Isometries of the Plane

Translation

A *translation* of a plane figure shifts the figure in a given direction. Under a translation, there are no fixed points; every point moves by exactly the same distance, *d*.

@ @ @ @

Fig 1.2.1 Horizontal translation

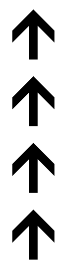

Fig 1.2.2 Vertical translation

Note that a translation need not take place horizontally or vertically. It can take place in any direction.

Reflection

A *reflection* is a mapping of all points of the original figure onto the other side of a "mirror line" such that the distance between the image (the figure that is mapped from the original one) and the mirror line is the same as that between the original figure and the mirror line. The mirror line is known as the *axis of reflection*.

Fig 1.2.3a

The above figure is obtained by reflecting the  in the vertical reflection axis:

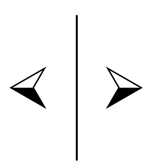

Fig 1.2.3b Reflection about a vertical axis.

Reflection can also take place in the horizontal axis as shown below:

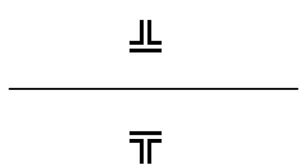

Fig 1.2.4 Reflection about a horizontal axis

In fact, the reflection axis needs not be a vertical line or a horizontal line; it can be any straight line at any angle to the horizontal.

For example,

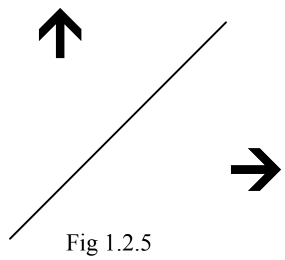

Fig 1.2.5

Rotation

We completely specify a *rotation* when we know its *centre* and *angle of rotation*. A figure with an angle of rotation θ is said to have an *order of rotation n* if $n = 360^{\circ}/\theta$ and n is a natural number. We define a *symmetry region* as a subset of the figure which generates the whole figure by rotations.

The table below illustrates the concepts of angle, order and centre of rotation. Please refer to the explanation beneath the table to understand what is illustrated in the table.

Order of Rotation	Angle of Rotation	Figure	Symmetry Regions
2	180°	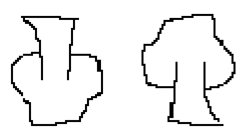 1.2.6a	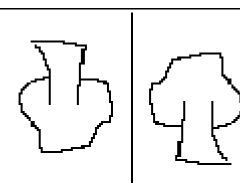 1.2.6b
3	120°	 1.2.7a	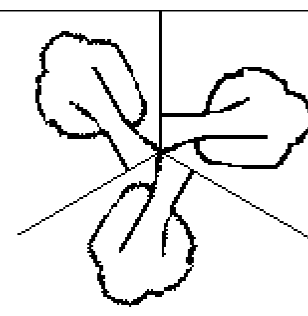 1.2.7b

Order of Rotation	**Angle of Rotation**	**Figure**	**Symmetry Regions**
4	90^{o}	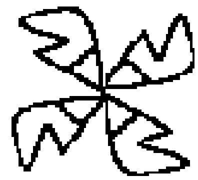 1.2.8a	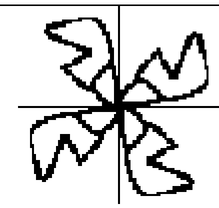 1.2.8b
6	60^{o}	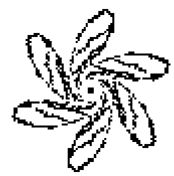 1.2.9a	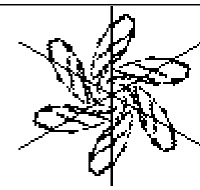 1.2.9b

Table 1.2.1

For each figure in the third column, we obtain information about its angle of rotation by drawing lines as shown in the forth column. The lines show three details:

1) The lines divide the figure into smaller regions, such that each region is identical (except in the orientation of the figure in each region) and each region is the smallest possible such that sufficient rotations of it will generate the whole figure. The number of such regions as partitioned by the lines will give the *order of rotation* of the figure.

2) The angle of intersection of the lines shows the *angle of rotation*.

3) The point of intersection of the lines shows the *centre of rotation*.

Note that for Fig 1.2.6a, there is only one line dividing the figure. This line divides the figure into two identical regions (apart from the orientation of the figure in each region), so the order is two and the angle of rotation is 180^{o}. Now, the question is: where is the centre of rotation since there is no intersection of lines? Take a point *p* in the original figure and locate the image of *p*. Call this image *p'*. Draw the line *pp'* and the midpoint of this line is the centre of rotation of the figure.

Glide Reflection

A *glide reflection* is a combination of two transformations: a reflection and a translation. Whether the original figure is reflected or translated first does not affect the final result; the final figure generated will be the same.

Consider the following figure, in which the original figure is .

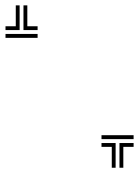

Fig 1.2.10

Let us try to obtain Figure 1.2.10 from  using two methods, which differ only in the sequence of reflection and translation transformations.

First Method : Reflection first, then translation

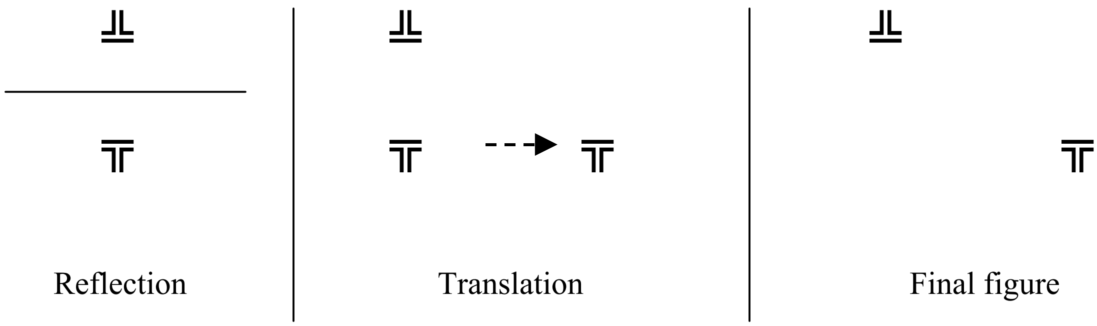

Second Method : Translation first, then reflection

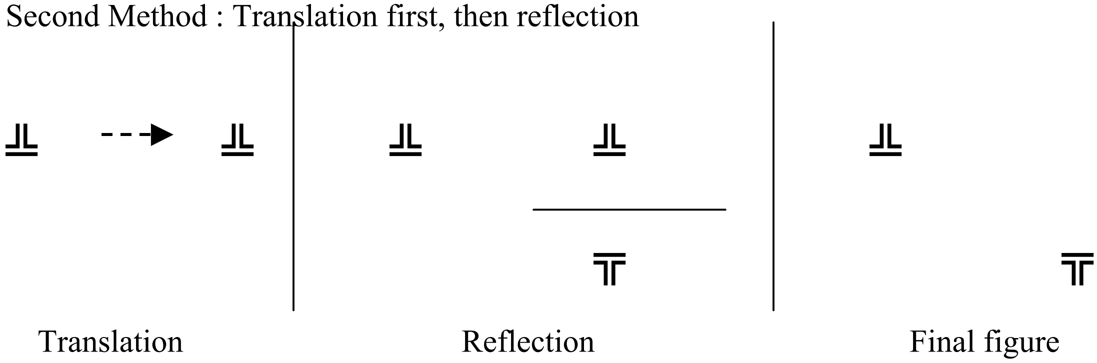

A glide reflection is *non-trivial* if its translation component and reflection component are not symmetries of the figure. We say a figure admits a glide reflection if and only if the glide reflection is non-trivial. The *glide reflection axis* is the axis of its reflection component.

We are done with the description of the four transformations.

1.3 Designs, Patterns, Motifs and Fundamental Regions

In our context, we will call figures with at least one (non-trivial[1]) symmetry *designs*. We will call designs that have a translation symmetry *patterns*. Note that patterns are unbounded figures, since with translation, the figures must extend to infinity. We will be concerned with only two types of patterns, namely *frieze patterns* which admit translation in only one direction and *wallpaper patterns* which admit translations in two or more directions. In particular, each pattern has a *basic unit* which is a smallest region of the plane such that the set of its images under translations of the pattern generates the whole pattern. Finally, we call designs that do not admit translation symmetry *finite designs*. Note that since the square of a glide reflection is a translation, therefore a finite design can only admit rotation and reflection symmetries.

a b

Fig 1.3.1 Examples of finite designs

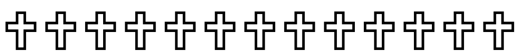

Fig 1.3.2 A frieze pattern

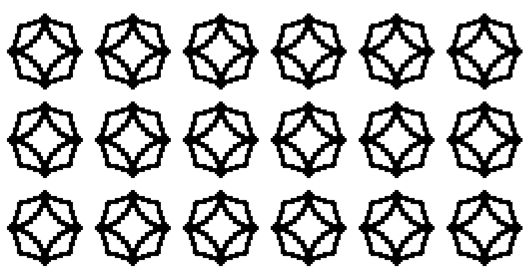

Fig 1.3.3 A wallpaper pattern

Some comments have to be made about Figures 1.3.2 and 1.3.3. Though by definition patterns extend to infinity, it is not possible in real life to have infinitely many translations of a figure. Therefore, as a general rule, we consider a figure to be a frieze pattern if it has at least the basic unit and a copy of it by translation. For a plane figure to qualify as a wallpaper pattern, it must have at least the basic unit, one copy by translation, and a copy of these two by translation in a second direction. There must be at least two rows, each one at least two units long. Hence, it can be seen easily that Figure 1.3.2 is a frieze pattern with  as a basic unit and Figure 1.3.3 is a wallpaper pattern with the basic unit .

[1] The trivial symmetry is the identity transformation, which maps the figure back to itself.

Let us now discuss the generation of a wallpaper pattern. Within each basic unit, we can find a smallest region in the basic unit whose images under the full symmetry group of the pattern cover the plane. This smallest region is known as a *fundamental region*. If the pattern consists of a figure on a plain background, we can instead focus on the part of the figure that generates the pattern. A *motif* is a subset of a fundamental region which has no symmetry but which generates the whole pattern under the symmetry group of the pattern. To understand the difference between a fundamental region and a motif, think of the fundamental region as a region, which together with the symmetry group, determines the structure of the patterns. The motif on the other hand, determines the appearance of the pattern. To make the idea clearer, let us use Figure 1.3.3 to illustrate what is a fundamental region and a motif.

Firstly, observe that the symmetry group of Figure 1.3.3 comprises vertical reflection, horizontal reflection, reflection with axis at 45^o clockwise from horizontal, reflection at 135^o clockwise from horizontal, 90^o rotation, vertical translation and horizontal translation. A fundamental region of this wallpaper pattern is a triangular region  with the motif . So the fundamental region is indeed . Note that the grey shading of the triangular fundamental region has no role in the generation of the pattern; the shading is done to allow the reader to see the shape of the fundamental region. The following sequence of steps is just one of the ways the region can generate the pattern.

1) Reflect  horizontally to form 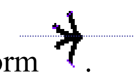.
2) Rotate by 90^o to form  where the dot represents the center of rotation.
3) Reflect about the axis that is 135^o counter-clockwise from horizontal to form 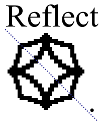. So we get a unit of the pattern.
4) Translate the unit vertically and horizontally and we get the desired pattern.

1.4 Symmetry Groups of Finite Designs

Recall that a *finite design* is a figure that

1) has at least one of rotation symmetry or reflection symmetry
2) does not have translation symmetry.

We can categorise finite designs into two classes of symmetry groups C_n and D_n. C_n refers to cyclic groups of order n. Designs which fall into type C_n are those which have rotation of order n but no reflection symmetry. On the other hand, D_n refers to dihedral groups of order n. Designs which fall into type D_n have exactly n distinct reflection axes and rotation of order n.

A note of caution though: C_1 is the group for a finite figure which has no symmetry at all- neither rotational nor reflection. D_1 is the group for designs which have reflection symmetry but no other symmetries.

Examples of designs in cyclic groups are shown in Table 1.2.1:

Fig 1.2.6a is of C_2,
Fig 1.2.7a is of C_3,
Fig 1.2.8a is of C_4,
Fig 1.2.9a is of C_6.

We can have designs in C_{50}, C_{999}, or of even higher orders! Therefore, cyclic groups form an infinite class.

Let us now move on to dihedral groups. The following table illustrates some examples of designs in dihedral groups.

Order of Dihedral Group	Figure	Figure with Reflection Lines
1	 1.4.1a	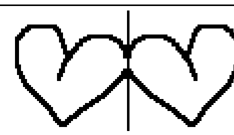 1.4.1b
2	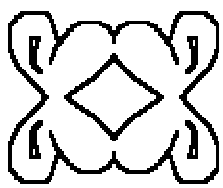 1.4.2a	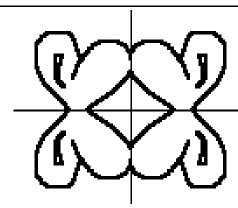 1.4.2b
3	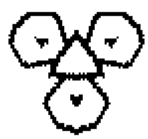 1.4.3a	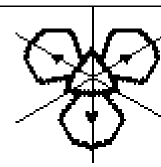 1.4.3b
6	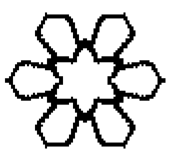 1.4.4a	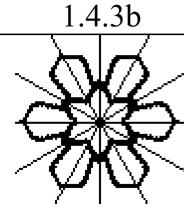 1.4.4b
8	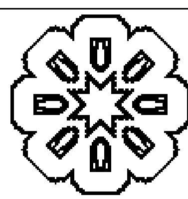 1.4.5a	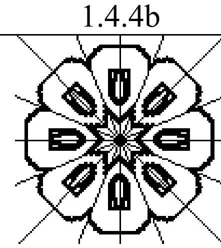 1.4.5b

Table 1.4.1

For each dihedral group, we analyse the rotational symmetries the way we do for cyclic designs. Observe that the reflection axes also partition the figure into the symmetry regions.

As in the case of cyclic groups, dihedral groups also form an infinite class.

1.5 Symmetry Groups of Frieze Patterns

Like finite designs, frieze patterns can also be classified according to the kinds of symmetries they admit. There are seven classes of frieze patterns. Unlike cyclic and dihedral groups which are infinite classes, there are only finite number of classes into which frieze patterns can be put into. The reader is invited to take a look at the proof in Appendix 2 of Washburn and Crowe **[1]**.

The symmetry groups of frieze patterns are named in the form of a four-symbol notation *pxyz*. Each name begins with the letter p. The following informs the reader how to derive the rest of the four-symbol notation for each symmetry group for frieze patterns.

x = { m   if there is vertical reflection
    { 1   otherwise

y = { m   if there is horizontal reflection
    { a   if there is a glide reflection but no horizontal reflection
    { 1   otherwise

z = { 2   if there is a half turn
    { 1   otherwise

We can also use a two-symbol notation *xy* proposed by Senechal (1975):

x = { m   if there is vertical reflection
    { 1   otherwise

y = { m   if there is horizontal reflection
    { g   if there is a glide reflection with no horizontal reflection
    { 2   if there is a half-turn with no glide nor horizontal reflection
    { 1   otherwise

The following table illustrates some examples of each of the seven symmetry groups for frieze patterns.

Symmetry Group 4-symbol/ 2-symbol	Figure	Figure with symmetry axes and centers of rotation as blue dots	Isometries present (besides translation)
pmm2 / mm	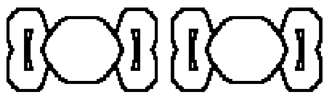 Fig 1.5.1a	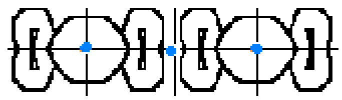 Fig 1.5.1b	vertical and horizontal reflections; 2-fold rotation[2]
pma2 / mg	 Fig 1.5.2a	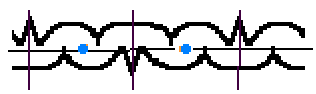 Fig 1.5.2b	vertical reflection; horizontal glide reflection; 2-fold rotation
pm11 / m1	 Fig 1.5.3a	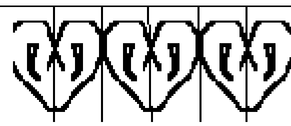 Fig 1.5.3b	only vertical reflection
p1m1 / 1m	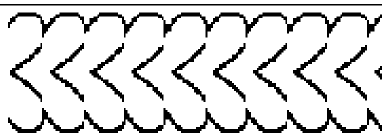 Fig 1.5.4a	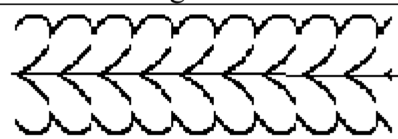 Fig 1.5.4b	only horizontal reflection
p1a1 / 1g	 Fig 1.5.5a	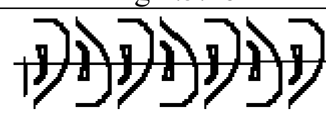 Fig 1.5.5b	only horizontal glide reflection
p112 / 12	 Fig 1.5.6a	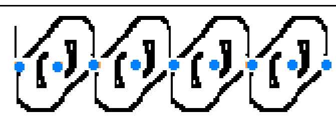 Fig 1.5.6b	only 2-fold rotation.
p111 / 11	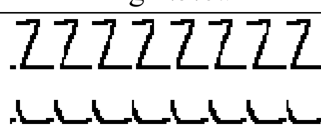 Fig 1.5.7a	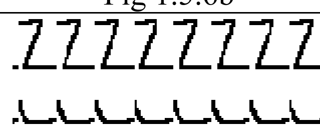 Fig 1.5.7b	No other symmetry except translation.

Table 1.5.1

[2] A 2-fold rotation is a rotation of order 2. In general, a *n-fold rotation* is a rotation of order n.

An Approach to Analyse the Symmetry Groups of Frieze Patterns

I would recommend the use of the following flow chart to analyse the symmetry groups of frieze patterns.

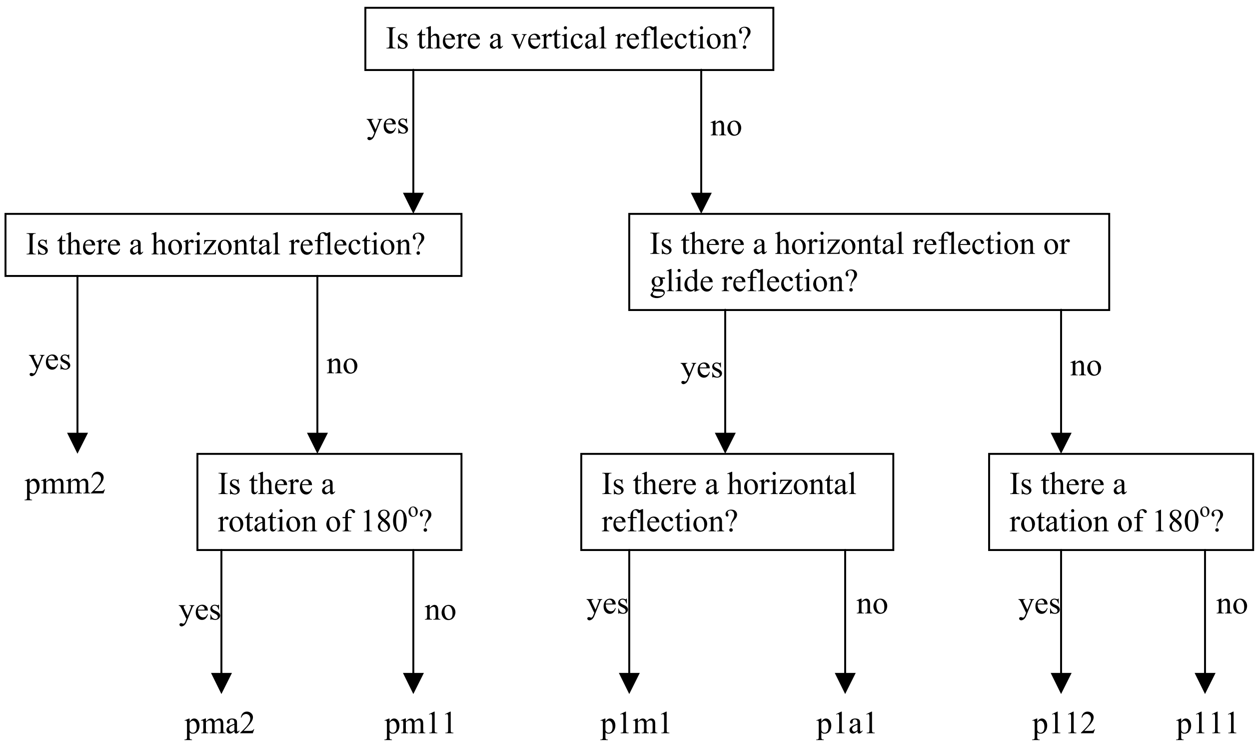

Chart 1.5.1 Flow chart for the 7 symmetry groups of frieze patterns

1.6 Symmetry Groups of Wallpaper Patterns

Before we go on to discuss the symmetry groups of wallpaper patterns, we need to learn about *lattices of points* and *primitive cells* of the patterns. We obtain a lattice of points of a wallpaper pattern by the following method:

1) Start by choosing a point p. If the pattern admits rotations, then p is a centre of rotation of the highest order. If the pattern does not have rotational symmetry, then p is any arbitrary point in the pattern.
2) Apply translations of the pattern on p. The set of all images of p under the translations form the lattice.

A *primitive cell* is a parallelogram such that the following hold:

1) Its vertices are lattice points.
2) It contains no other lattice points inside it or on its edge.
3) The vectors which form the sides of this parallelogram generate the translation group of the pattern.

There are only five types of primitive cells: parallelogram, rectangular, square, rhombic and hexagonal (the hexagonal cell is a rhombus consisting of two equilateral triangles). A descriptive proof is given by Schattschneider **[2]**.

To determine which cell the pattern actually takes, we need to obtain a lattice of points and form a parallelogram whose vertices are lattice points and whose interior and edges have no other lattice points. Sometimes, we get more than one type of parallelogram using the way just described. When such circumstances arise, we need a way to choose which parallelogram is the primitive cell. Below is a method to determine what is the primitive cell of each wallpaper pattern.

1) A pattern with order of rotation three or six takes a hexagonal cell.
2) A pattern with order of rotation four takes a square cell.
3) For a pattern with order of rotation one or two,
    i) if there is neither reflection nor glide reflection, then it takes a parallelogram.
    ii) otherwise, it takes either a rectangular cell or a rhombic cell. Plot the lattice and draw a parallelogram as described initially.
        a) It takes a rectangular cell if the four corners of the primitive cell are right angles.
        b) Otherwise, it takes a rhombic cell.

The following table illustrates the lattice of points and the primitive cell.

Figure	**Lattices (green dots) with primitive cell (in purple)**	**Type of primitive cell**
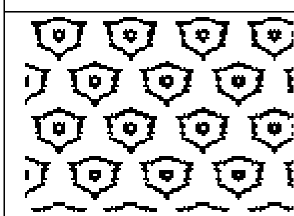 1.6.1a	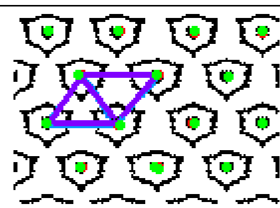 1.6.1b	Hexagonal (Observe that it is made up of 2 equilateral triangles.)
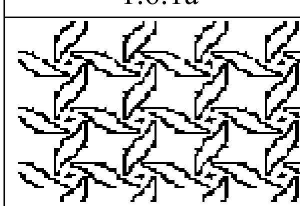 1.6.2a	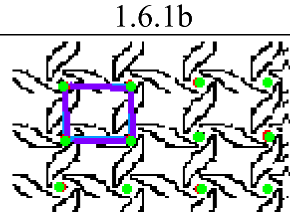 1.6.2b	Square
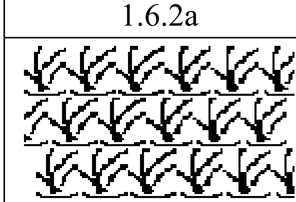 1.6.3a	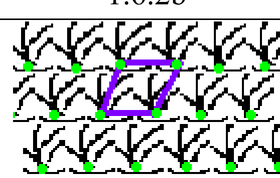 1.6.3b	Parallelogram

Figure	**Lattices (green dots) with primitive cell (in purple)**	**Type of primitive cell**
 1.6.4a	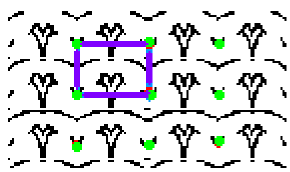 1.6.4b	Rectangular
 1.6.5a	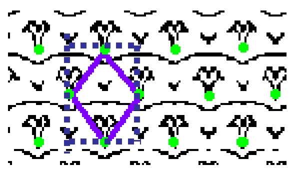 1.6.5b	Rhombic

Table 1.6.1

Note that for a rhombic cell, we extend it to a rectangle as shown dotted in the above table. This extended cell is known as a *centred cell*. The notion of the centred cell is useful only in the notation of the symmetry groups of wallpaper patterns.

Now, we are ready to talk about the symmetry groups of wallpaper patterns. The names for the symmetry groups describing wallpaper patterns, like the frieze patterns, adopt a four-symbol notation *qrst*. The notation comes from crystallographers who use it to classify crystals. The interpretation of the crystallographic notation is as follows:

q = { p if the primitive cell is not a centred cell
{ c if the primitive cell is a centred cell

r = n, the highest order of rotation

s denotes a symmetry axis normal to the left edge of the primitive or centred cell
This left edge is known as the *x-axis*.
s = { m if there is a reflection axis
{ g if there is no reflection axis, but a glide-reflection axis
{ 1 if there is no symmetry axis

t denotes a symmetry axis at angle θ ($\leq 180^o$) to the x-axis.
In particular, $\theta = 180^o$ if n = 1 or 2 ; $\theta = 45^o$ if n = 4 ; $\theta = 60^o$ if n = 3 or 6.
t = { m if there is a reflection axis
{ g if there is no reflection, but a glide-reflection axis
{ 1 if there is no symmetry axis

No symbols in the third and forth positions indicate that the group contains neither reflections nor glide-reflections.

Some comments have to be made about the left edge of the cell that is known as the *x-axis*. Recall in 3-dimensional space with (x,y,z) co-ordinate system, the x-axis is the axis that points towards the reader. In other words, the x-axis is the left axis in the horizontal x-y plane. Hence, defining the left edge of cells as the x-axis makes sense to the crystallographers who deal with symmetry groups of 3-dimensional objects. However, here, we are dealing with the groups for 2-dimensional patterns. The x-axis in our wallpaper patterns is not necessarily the literal left edge of the primitive cells. To get the x-axis of the primitive cell of a wallpaper pattern requires the pattern to be aligned in a certain way or choosing the primitive cell in a certain way. For example, observe the following figures and decide what is the left edge of the primitive cell.

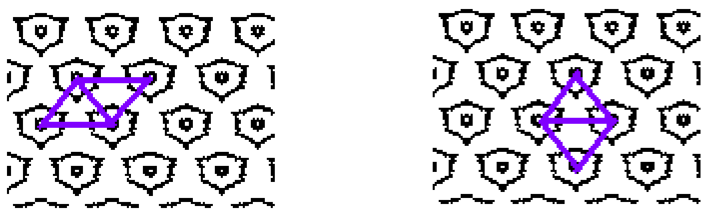

a b

Fig 1.6.6 Choosing the hexagonal primitive cell in different ways for the same pattern

For Figure 1.6.6a, it is easy to see where is the left edge of the cell, but for Figure 1.6.6b, it is ambiguous where the left edge is! I suggest the following way to determine the x-axis, the third symbol and the forth symbol of the notation of the symmetry groups.

1) Draw the primitive cell. If it is a rhombic cell, replace it by a centred cell.

2) i) If there is a reflection that is perpendicular to an edge of the cell, that edge is the x-axis and the third symbol is *m*.

   ii) Otherwise, if there is a glide reflection axis that is perpendicular to an edge of the cell, that edge is the x-axis and the third symbol is *g*.

   iii) Otherwise, any edge is the x-axis and the third symbol is *1*.

3) If there is a reflection or glide reflection axis that is not normal to the x-axis, then the forth symbol is m or g respectively. Otherwise, the forth symbol is 1.

The table on the following pages illustrates examples of wallpaper patterns for each symmetry group. In all, there are seventeen wallpaper symmetry groups.

Notation For Symmetry Group (4-symbol / short form)	**Figure**	**Figure with primitive cell (in purple) symmetry axis (in dark green) centre of rotation (green dot)**	**Remarks on deriving the correct symmetry group (Note: let a glide reflection be denoted as a glide for convenience)**
c1m1/cm	 1.6.6a	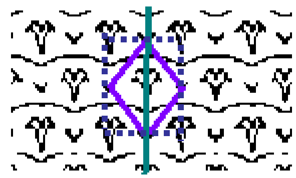 1.6.6b	Centred cell. There is a reflection axis normal to the horizontal edges of the centred cell. Pick one of these 2 edges as the x-axis. So the 3rd symbol is m. No other symmetry.
p1m1/pm	 1.6.7a	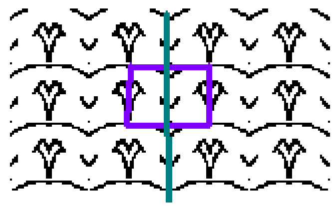 1.6.7b	Rectangular cell. There is a reflection axis normal to the horizontal edges of the cell. Pick one of these 2 edges as the x-axis. So the 3rd symbol is m. No other symmetry.
p1g1/pg	 1.6.8a	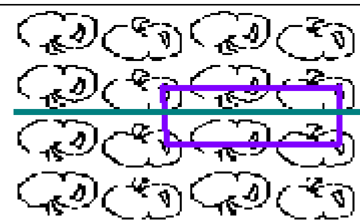 1.6.8b	Rectangular cell. No reflection axes. There is a glide axis normal to the vertical edges of the cell. Pick one of these 2 edges as the x-axis. So the 3rd symbol is g. No other symmetry.

Notation For Symmetry Group (4-symbol / short form)	**Figure**	**Figure with primitive cell (in purple) symmetry axis (in dark green) centre of rotation (green dot)**	**Remarks on deriving the correct symmetry group (Note: let a glide reflection be denoted as a glide for convenience)**
p1/p1	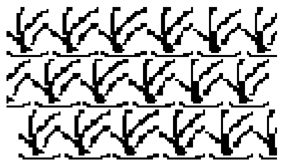 1.6.9a	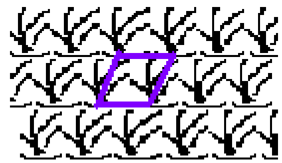 1.6.9b	Parallelogram cell. No other symmetry besides translations.
p2mg/pmg	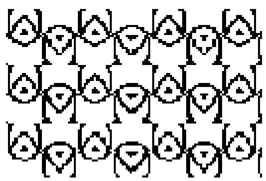 1.6.10a	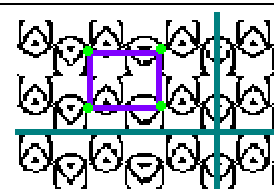 1.6.10b	Rectangular cell. 2-fold rotation. There is a reflection axis normal to the horizontal edges of the cell. Pick one of these 2 edges as the x-axis. So the 3rd symbol is m. There is a glide axis parallel to the x-axis. So the 4th symbol is g.
p2mm/pmm	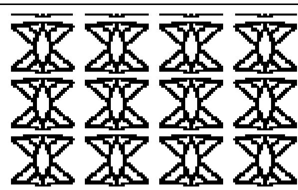 1.6.11a	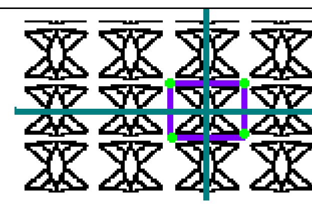 1.6.11b	Rectangular cell. 2-fold rotation. Both reflection axes are normal to some edges of the cell. So the x-axis is any of the edges and both the 3rd and 4th symbols are m.
c2mm/cmm	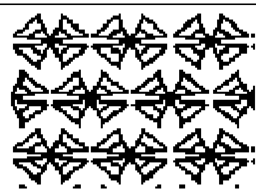 1.6.12a	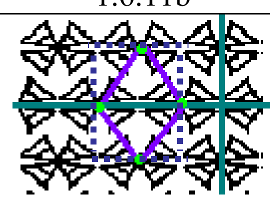 1.6.12b	Centred cell. 2-fold rotation. Both reflection axes are normal to some edges of the centred cell. So the x-axis is any of the edges and both the 3rd and 4th symbols are m.

Notation For Symmetry Group (4-symbol / short form)	Figure	Figure with primitive cell (in purple) symmetry axis (in dark green) centre of rotation (green dot)	Remarks on deriving the correct symmetry group (Note: let a glide reflection be denoted as a glide for convenience)
p2gg/pgg	 1.6.13a	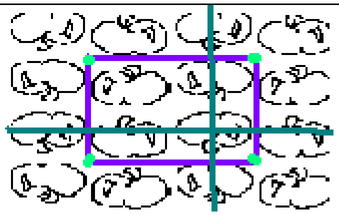 1.6.13b	Rectangular cell. 2-fold rotation. No reflection. Both glide axes are normal to some edges of the cell. So the x-axis is any of the edges and both the 3rd and 4th symbols are g.
p211/p2	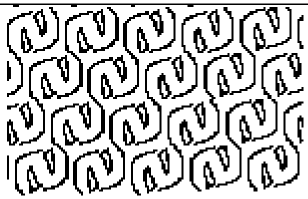 1.6.14a	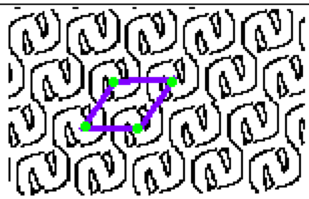 1.6.14b	Parallelogram cell. 2-fold rotation. No other symmetry.
p4/p4	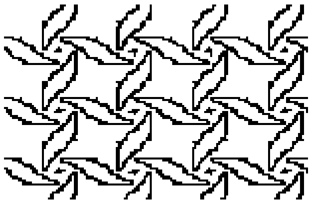 1.6.15a	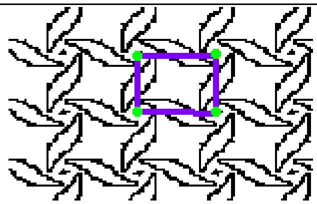 1.6.15b	Square cell. 4-fold rotation. No other symmetry.

Notation For Symmetry Group (4-symbol / short form)	**Figure**	**Figure with primitive cell (in purple) symmetry axis (in dark green) centre of rotation (green dot)**	**Remarks on deriving the correct symmetry group (Note: let a glide reflection be denoted as a glide for convenience)**
p4mm/p4m	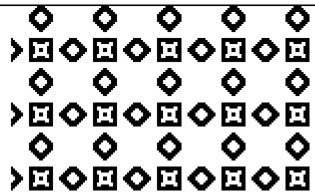 1.6.16a	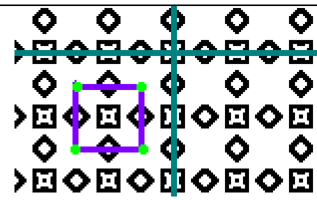 1.6.16b	Square cell. 4-fold rotation. Both reflection axes are normal to some edges of the cell. So the x-axis is any of the edges and both the 3rd and 4th symbols are m.
p4gm/p4g	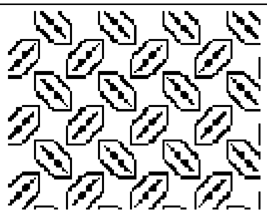 1.6.17a	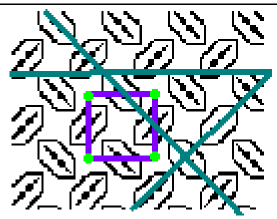 1.6.17b	Square cell. 4-fold rotation. No reflection axis that is normal to any edges of the cell. There is a glide axis normal to the vertical edges of the cell. Pick one of these 2 edges as the x-axis. So the 3rd symbol is g. There is a reflection axis that is not normal to the x-axis. So the 4th symbol is m.
p3/p3	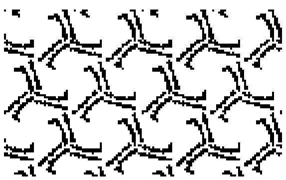 1.6.18a	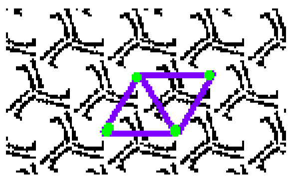 1.6.18b	Hexagonal cell. 3-fold rotation. No other symmetry.

Notation For Symmetry Group (4-symbol / short form)	**Figure**	**Figure with primitive cell (in purple) symmetry axis (in dark green) centre of rotation (green dot)**	**Remarks on deriving the correct symmetry group (Note: let a glide reflection be denoted as a glide for convenience)**
p3m1/ p3m1	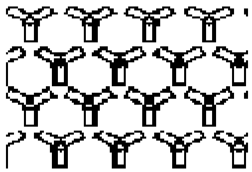 1.6.19a	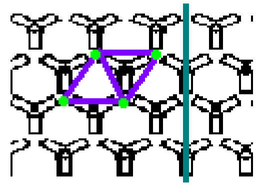 1.6.19b	Hexagonal cell. 3-fold rotation. There is a reflection axis normal to the horizontal edges of the cell. Pick one of these 2 edges as the x-axis. So the 3rd symbol is m. No other symmetry.
p31m/ p31m	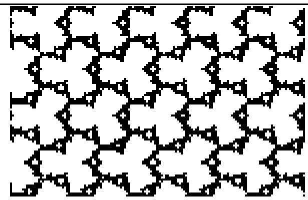 1.6.20a	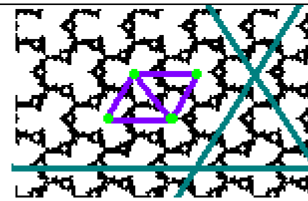 1.6.20b	Hexagonal cell. 3-fold rotation. No reflection or glide axis that is normal to any edges of the cell. So the 3rd symbol is 1. There is a reflection axis not normal to all edges. So the 4th symbol is m.
p6/p6	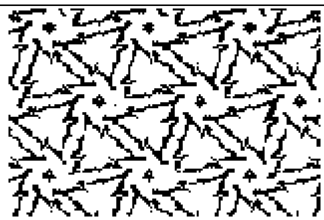 1.6.21a	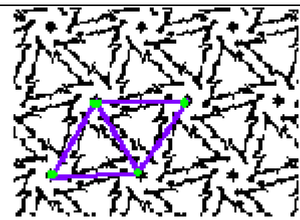 1.6.21b	Hexagonal cell. 6-fold rotation. No other symmetry.

Notation For Symmetry Group (4-symbol / short form)	**Figure**	**Figure with primitive cell (in purple) symmetry axis (in dark green) centre of rotation (green dot)**	**Remarks on deriving the correct symmetry group (Note: let a glide reflection be denoted as a glide for convenience)**
p6mm/p6m	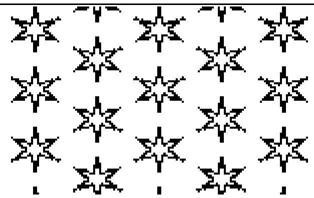 1.6.22a	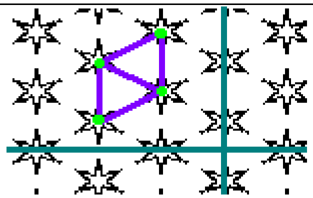 1.6.22b	Hexagonal cell. There is a reflection axis normal to the vertical edges of the cell. Pick one of these 2 edges as the x-axis. So the 3rd symbol is m. There is a reflection axis not normal to the x-axis. So the 4th symbol is m.

Table 1.6.2

An Approach to Analyse the Symmetry Groups of Wallpaper Patterns

Like frieze patterns, we can use flow charts to determine the symmetry groups of the wallpaper patterns. Here, we will give two flow charts. The first chart is from Washburn and Crowe **[1]** and the second chart is a modification of the first. The differences in the charts are highlighted in yellow in the second chart. Explanatory notes are given after the second chart.

Chart 1.6.1 First Flow Chart for the Symmetry Groups of Wallpaper Patterns

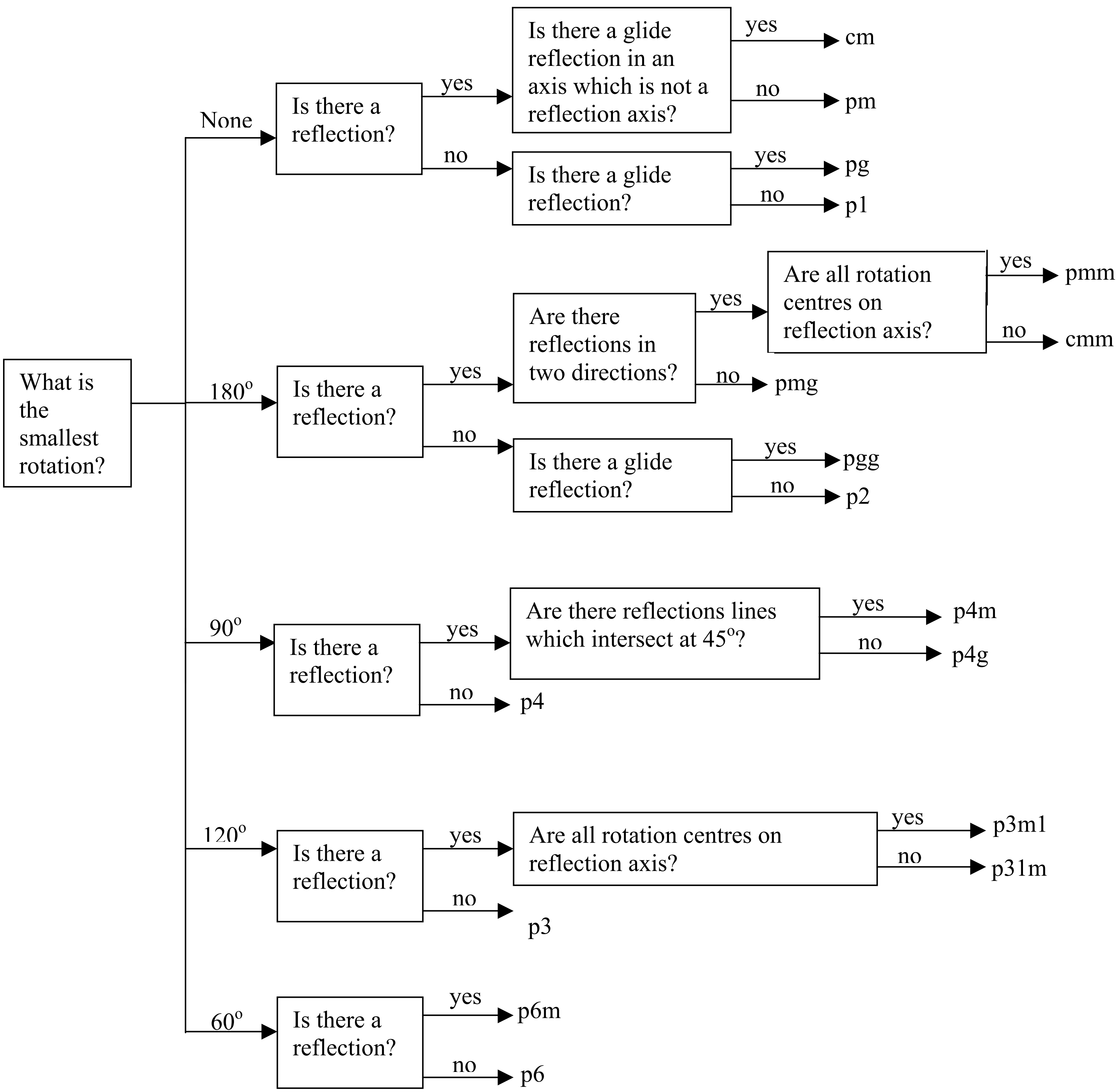

Chart 1.6.2 Second Flow Chart for the Symmetry Groups of Wallpaper Patterns

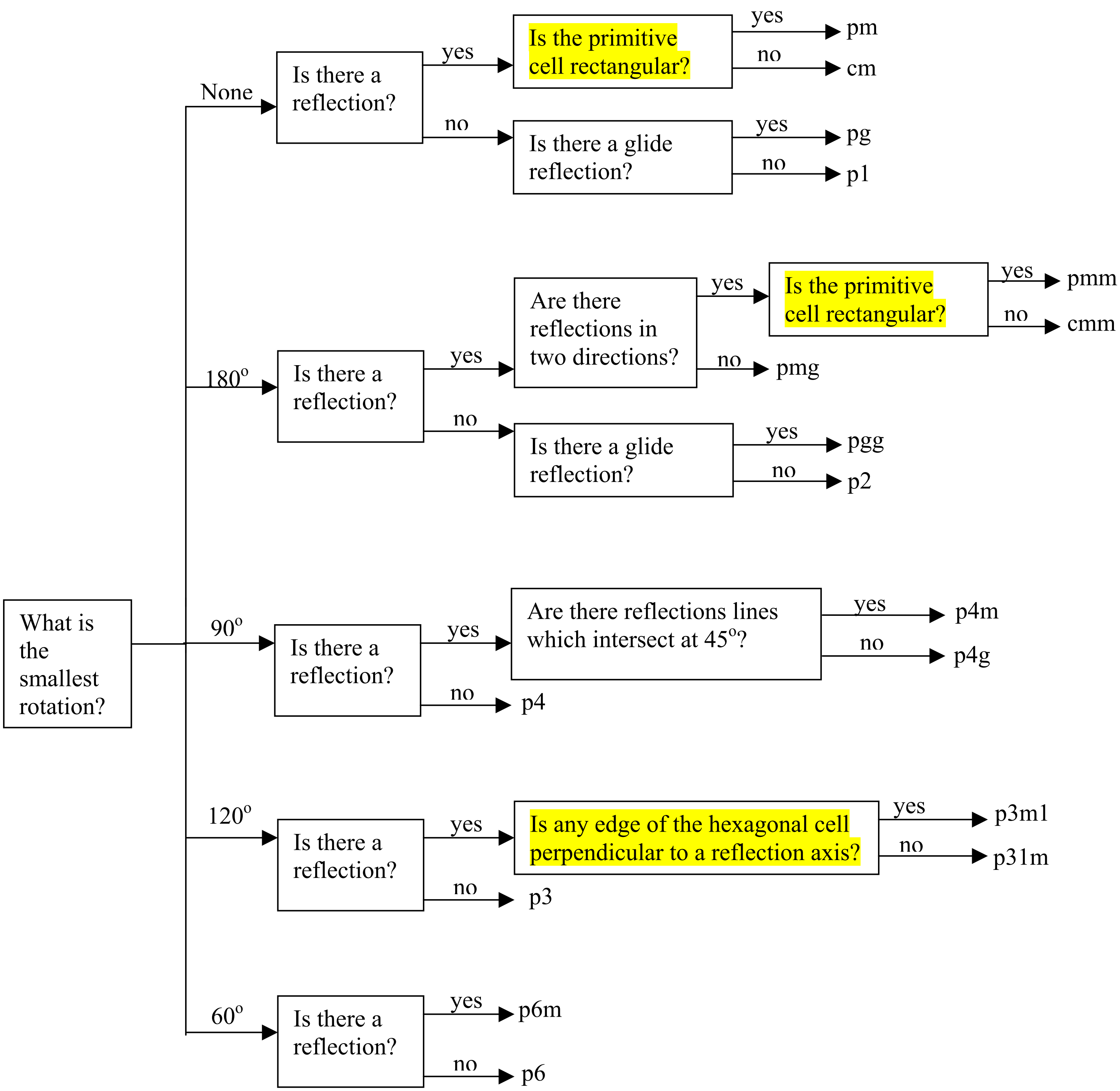

Examples to Illustrate the Difference in Approach in Each Flow Chart

(I) *cm* patterns versus *pm* patterns

Fig 1.6.23

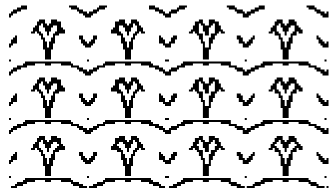

Fig 1.6.24

Steps to determine the correct symmetry group of Figures 1.6.23 and 1.6.24 using the charts:

1) Determine the smallest rotation. Both have no rotations.
2) Both have a vertical reflection.
3) a)Using Chart 1.6.1, to check for glide reflections and reflections:

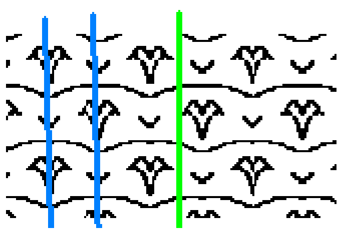

Fig 1.6.23a

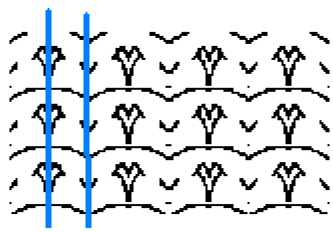

Fig 1.6.24a

The blue axes denote reflection axes and the green axis denotes a glide axis. Hence, Figure 1.6.23 is a *cm* pattern while Figure 1.6.24 is a *pm* pattern.

b) Using Chart 1.6.2, to check the primitive cells:

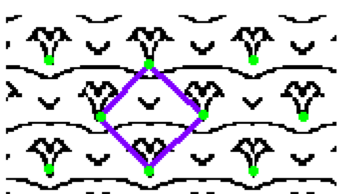

Fig 1.6.23b

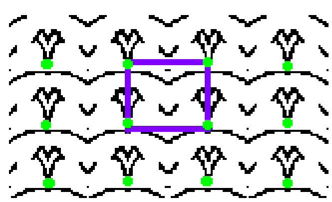

Fig 1.6.24b

The green dots form the lattice points of the figures. The blue parallelograms form the primitive cells. Hence, Figure 1.6.23 is a *cm* pattern while Figure 1.6.24 is a *pm* pattern.

(II) *cmm* patterns versus *pmm* patterns

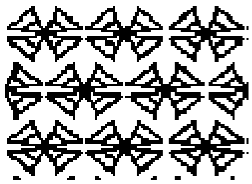
Fig 1.6.25

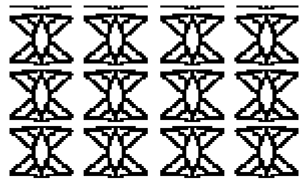
Fig 1.6.26

Steps to determine the correct symmetry group of Figures 1.6.25 and 1.6.26 using the charts:

1) Determine the smallest rotation. Both have rotations of 180^o.
2) Both have vertical and horizontal reflections.
3) a) Using Chart 1.6.1, to check for all rotation centres and reflection axes:

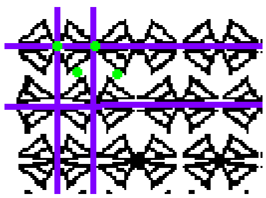
Fig 1.6.25a

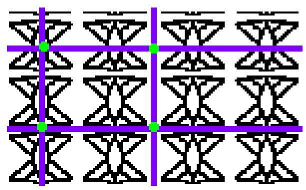
Fig 1.6.26a

The blue axes denote reflection axes and the green dots denote rotation centres. In Figure 1.6.25, some rotation centres are not on reflection axes but in Figure 1.6.26, all rotation centres are on reflection axes. So, Figure 1.6.25 is of class *cmm* while Figure 1.6.26 is of class *pmm*.

b) Using Chart 1.6.2, to check the primitve cells:

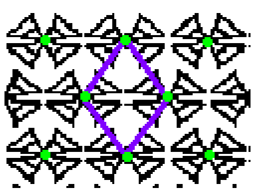
Fig 1.6.25b

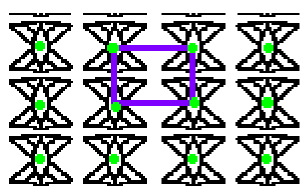
Fig 1.6.26b

The green dots in the above figures denote lattice points and the blue parallelograms denote primitive cells. Hence Figure 1.6.25 is a *cmm* pattern while Figure 1.6.26 is a *pmm* pattern.

(III) *p31m* patterns versus *p3m1* patterns

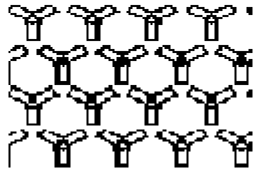

Fig 1.6.27

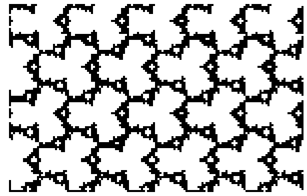

Fig 1.6.28

Steps to determine the correct symmetry group of Figures 1.6.25 and 1.6.26 using the charts:

1) Determine the smallest rotation. Both have rotations of 120^{o}.
2) Both have reflection. Figure 1.6.27 has a vertical reflection while Figure 1.6.28 has a horizontal reflection.
3) a) Using Chart 1.6.1, to check for rotation centres and reflection axes:

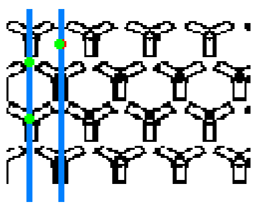

Fig 1.6.27a

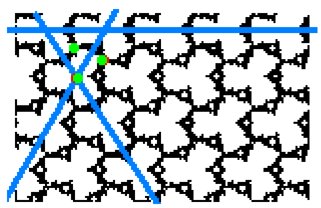

Fig 1.6.28a

The blue axes denote reflection axes and the green dots denote rotation centres. So Figure 1.6.27 is a *p3m1* pattern while Figure 1.6.28 is a *p31m* pattern.

b) Using Chart 1.6.2, to check if any edge of the hexagonal cell is perpendicular to any reflection axes:

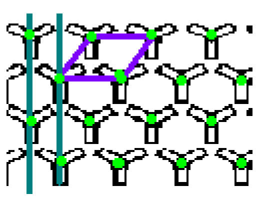

Fig 1.6.27b

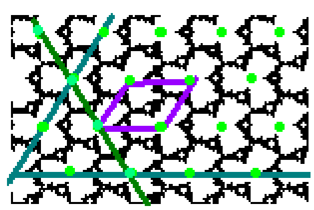

Fig 1.6.28b

The blue parallelograms are the primitive cells while the dark green lines denote reflection axes. The light green dots denote lattice points. In Figure 1.6.27, the horizontal edge is perpendicular to a reflection axis while in Figure 1.6.28, none of the edges of the primitive cell is perpendicular to any reflection axes. Hence Figure 1.6.27 is a *p3m1* pattern while Figure 1.6.28 is a *p31m* pattern.

Alternative Approach to Determine *p31m* Patterns and *p3m1* Patterns

The two charts shown previously recommend two methods to determine *p31m* patterns and *p3m1* patterns. Here, we offer another method to tell the difference between the two patterns.

1) Select a type of rotation centre with a three-legged object.
2) Observe if the legs of this object point towards the centres of the nearest three-legged objects.
   If yes, then it is *p31m*. Otherwise, it is *p3m1*.

Let us use the methodology on Figures 1.6.27 and 1.6.28.

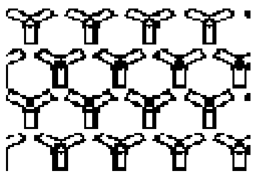

Fig 1.6.27

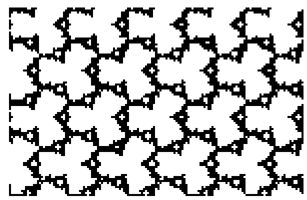

Fig 1.6.28

So for each figure, we select the rotation centre, shown as green dots and colour the "legs" of the three-legged object blue, as shown below.

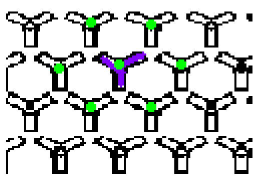

Fig 1.6.27c

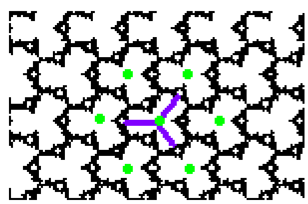

Fig 1.6.28c

For Figure 1.6.27c, the blue legs do not point towards the green dots, which represent the rotation centres of the blue-legged objects. For Figure 1.6.28c, the blue legs point towards the green dots. Hence, Figure 1.6.27 is of *p3m1* while Figure 1.6.28 is of *p31m*.

Chapter 2

Tilings

2.1 Introduction

Consider the following diagrams:

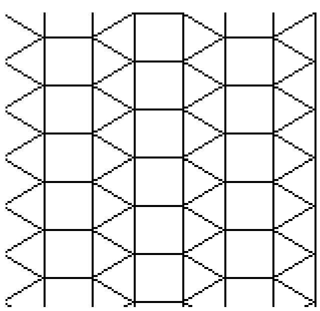

Fig 2.1.1

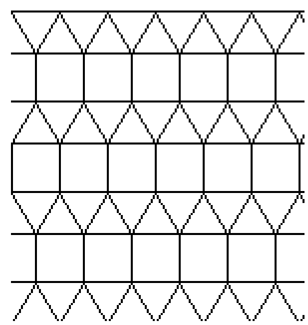

Fig 2.1.2

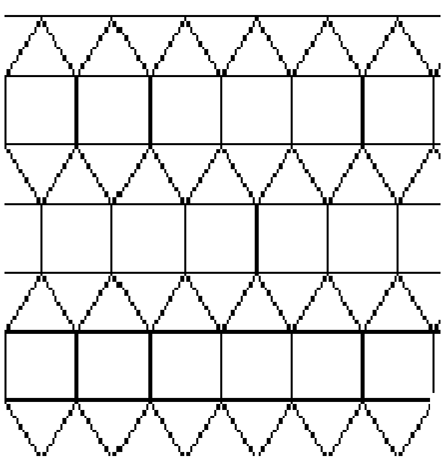

Fig 2.1.3

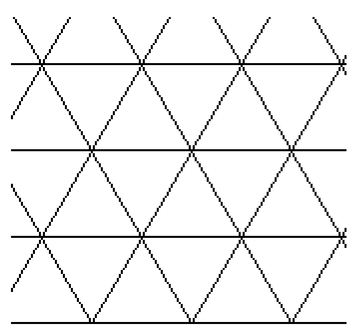

Fig 2.1.4

The diagrams above are known as *tilings* (or *tessellations*) of the plane. Observe that in each figure, we place pieces side by side without gaps and without overlaps. These pieces are known as *tiles* of the tiling. To be precise, a *tiling* of the plane is a countable family of closed sets T = {T_1, T_2,… } such that the union of T_1, T_2, …. is the whole plane and the interiors of the sets T_i are pairwise disjoint. Each T_i is known as a tile of T.

Two tilings T_1 and T_2 are said to be *congruent* if T_1 may be made to coincide with T_2 by an isometry of the plane. T_1 and T_2 are said to be *equal* if one of them can be changed on scale (magnified or contracted equally throughout the plane) so as to be congruent to the other. The main difference between being congruent and being equal is that to be congruent, T_1 and T_2 have to be of same size while to be equal, size does not matter. Referring to the above diagrams, Figures 2.1.1 and 2.1.2 are congruent; Figures 2.1.2 and 2.1.3 are equal; Figures 2.1.1 and 2.1.4 are not congruent.

A tiling T is *r-hedral* if there is a set $\mathcal{T}$ = {T_1, T_2,…T_r} of tiles such that:

1) each tile of T is congruent to exactly one tile from $\mathcal{T}$ and
2) each tile from $\mathcal{T}$ is congruent to at least one of the tiles of T.

Each $T_i \in \mathcal{T}$ is known as a *prototile*. The set of prototiles of a tiling is analogous to a basis for a vector subspace. Being *r*-hedral means that there are exactly *r* unique types of tiles which form the tiling T while for a *r*-dim subspace, there are exactly *r* linearly independent vectors which form the subspace.

In particular, a *monohedral tiling* is one that has only one prototile, a *dihedral tiling* has two prototiles and a *trihedral* tiling has three prototiles. Some examples of monohedral tilings are those formed by equilateral triangles, squares or regular hexagons as shown below:

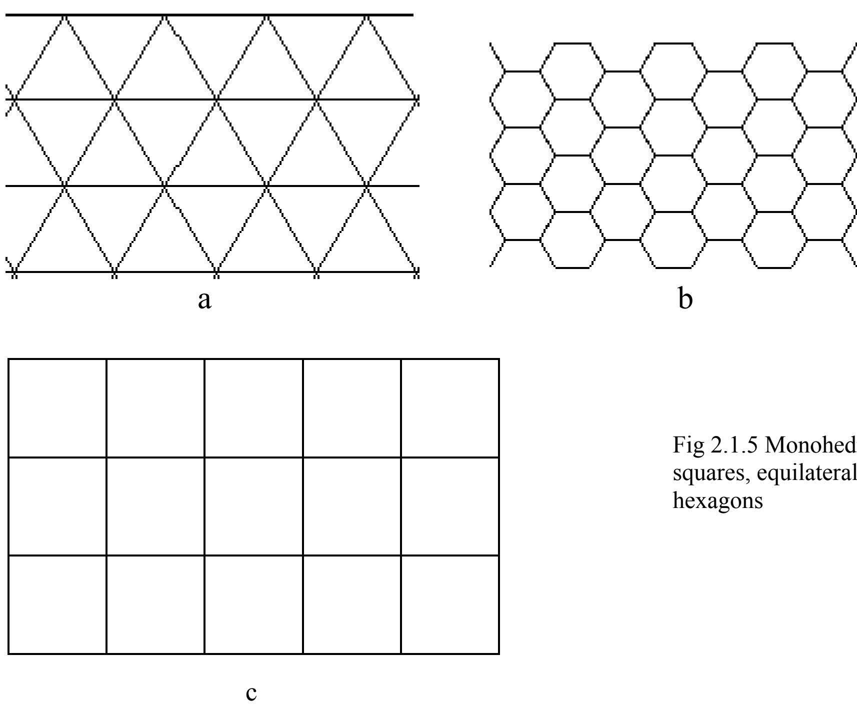

Fig 2.1.5 Monohedral tilings by squares, equilateral triangles, regular hexagons

An *edge-to-edge tiling* is a tiling such that each two tiles intersect along a common edge, only at a common vertex or not at all. In such a tiling, every side of every tile is an edge of the tiling and conversely. All the examples shown above are edge-to-edge tilings. In this chapter, we will consider only edge-to-edge tilings that are formed by regular polygons.

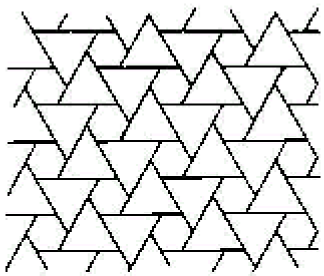

Fig 2.1.6 A tiling that is not edge-to-edge. Observe that each edge of the hexagons coincide with only half the edge of a triangular tile.

2.2 Edge-to-edge Tilings by Regular Polygons

Let us begin with some terminology associated with vertices in a tiling. The number of each kind of regular polygon surrounding a vertex determines the *species* of the vertex. We say the vertices in a tiling have the *same species* if all of them are surrounded alike in the number of each kind of regular polygon. Figure 2.2.1 shows two tilings whose vertices are all surrounded by three triangles and two squares. So we say that their vertices have the same species.

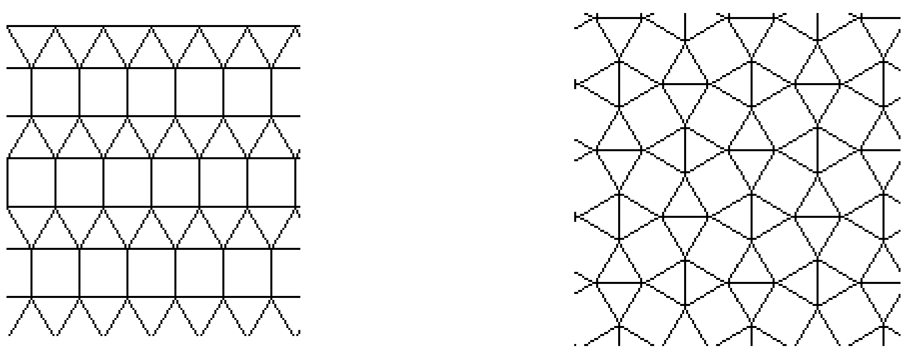

a b

Fig 2.2.1 Tilings with same species of vertices

A vertex is of *type* $n_1.n_2...n_r$ if it is surrounded in cyclic order by regular n-gons of order n_1, n_2,… and n_r. The cyclic order can be taken in any direction, be it clockwise or anti-clockwise. However, n_1 has to be of the lowest order of all polygons surrounding the vertex. In fact, in specifying the type of a vertex, $n_1.n_2...n_r$ has to be the sequence which is lexicographically first among all possible expressions. So Figure 2.2.1a shows a tiling whose vertices are all of type 3.3.3.4.4 (and not 3.4.4.3.3 or 3.3.4.4.3) while Figure 2.2.1b shows a tiling whose vertices are all of type 3.3.4.3.4 (and not 3.4.3.4.3). Therefore, the vertices in Figure 2.2.1a are of a different type from those in Figure 2.2.1b. Note that though the two tilings have vertices of the same species, they need not have vertices of the same type.

To make our notations neater, instead of labeling the type of vertex as 3.3.3.4.4, let us label it as $3^3.4^2$. Likewise for 3.3.4.3.4, we shorten the notation to $3^2.4.3.4$. The same applies to all other types of vertices.

As there are infinitely many edge-to-edge tilings by regular polygons, we shall restrict our study to those whose vertices have the same type. We will find out what is the total number of edge-to-edge tilings whose prototiles are regular polygons and whose vertices are of the same type.

First of all, let us determine what is the number of possible species of vertices. The interior angle of a regular n-gon is given by $^{180(n-2)}/_{n}$. Since the total number of degrees at a vertex is 360^o, we get the following equation:

$$360^o = \sum_{i=1}^{r} {}^{180(n_i-2)}/_{n_i}$$

n_i = order of the ith polygon in cyclic order
r = number of polygons surrounding the vertex
($r \leq 6$, since $n_i \geq 3$)

Solving the above equation, we get 17 solutions, that is we get 17 potential species of vertices, which give rise to 21 types of vertices. The following list shows the potential species:

1) 3.3.3.3.3.3
2) 3.3.3.3.6
3) i) 3.3.3.4.4 and ii) 3.3.4.3.4
4) i) 3.3.4.12 and ii) 3.4.3.12
5) i) 3.3.6.6 and ii) 3.6.3.6
6) i) 3.4.4.6 and ii) 3.4.6.4
7) 4.4.4.4
8) 3.7.42
9) 3.8.24
10) 3.9.18
11) 3.10.15
12) 3.12.12
13) 4.5.20
14) 4.6.12
15) 4.8.8
16) 5.5.10
17) 6.6.6

However, not all the species above form an edge-to-edge tiling. Some of them may leave gaps between tiles or overlap one another, which is not what we want. Let us now consider cases of vertex types that can give an edge-to-edge tiling.

Case 1 : If the type is 3.x.y

Let ABC be an equilateral triangle and suppose $x \leq y$. Consider the following diagram in which both vertices A and B are of type 3.x.y:

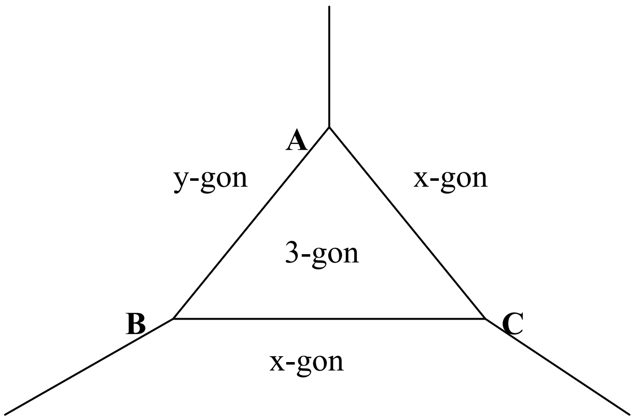

Fig 2.2.2

From the diagram, we can see that vertex C is of type 3.x.x.
Hence, if type 3.x.y is possible, then $x = y$ must hold.
So from the list, species 8, 9, 10 and 11 are not possible.

Case 2 : If the type is x.5.y

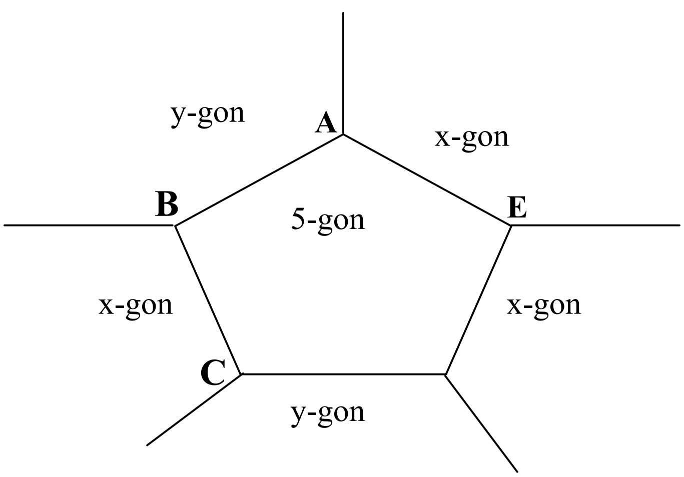

Fig 2.2.3

Consider a regular 5-gon ABCDE such that A, B, C and D are of type x.5.y, $x \leq 5 \leq y$.
Then, vertex E must be of type x.5.x, or rather, x.x.5.
So type x.5.y can give an edge-to-edge tiling if and only if $x = y$.
Therefore species 13 and 16 are not possible from the list.

Case 3 : If the type is 3.x.y.z

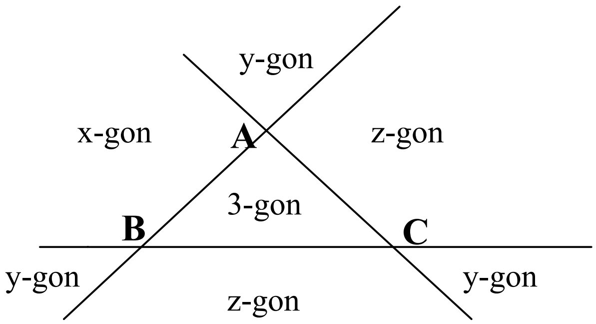

Fig 2.2.4a

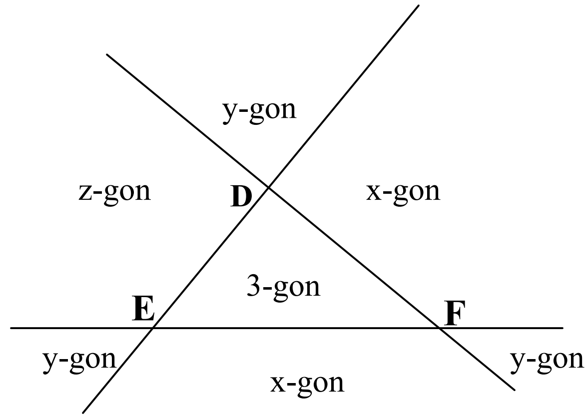

Fig 2.2.4b

Consider the regular 3-gons in Figures 2.2.4a and 2.2.4b. Suppose that vertices A, B, D and E are of type 3.x.y.z. For Figure 2.2.4a, vertex C then must take the type 3.z.y.z. For Figure 2.2.4b, vertex F must take 3.x.y.x. Hence, type 3.x.y.z can give an edge-to-edge tiling if and only if x = z. Therefore, species 4, 5i and 6i are not possible.

The rest of the species in the list can form edge-to-edge tilings. In all, there are eleven distinct edge-to-edge tilings by regular polygons such that all vertices are of the same type. Grunbaum and Shephard call these tilings *Archimedean* tilings. George D. Martin, however, calls only those that are non-monohedral edge-to-edge tilings by regular polygons Archimedean. In our context, we shall name the monohedral tilings as *Platonic* tilings while the non-monohedral ones as *Archimedean* tilings. These tilings are shown next page.

To fix our notation, vertex types will be labeled as w.x.y.z while tilings will be labeled as (w.x.y.z).

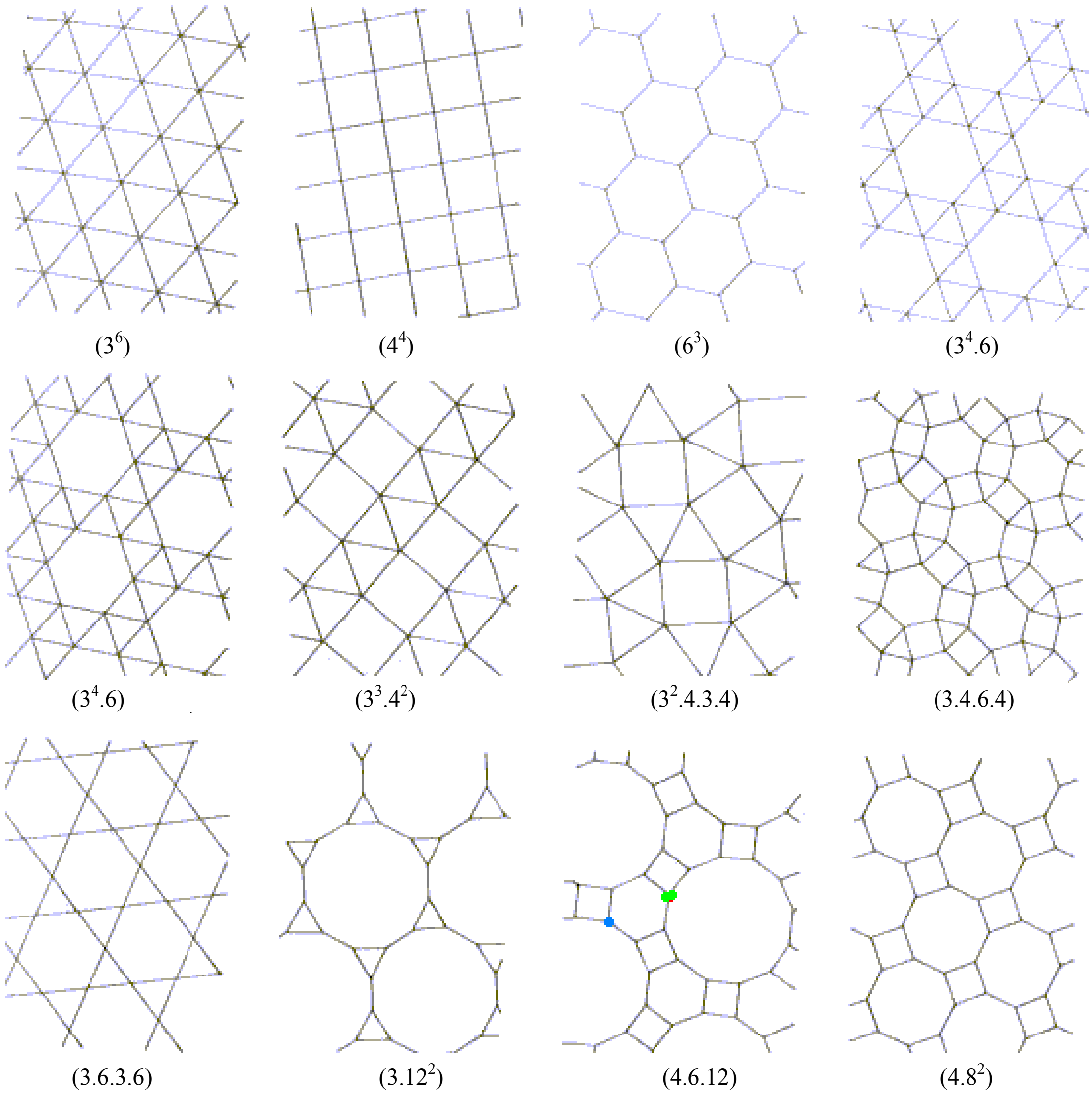

Fig 2.2.5 The eleven distinct types of tilings. The first three are Platonic tilings, the rest are Archimedean tilings. Notice that (3.4.6) occurs in two forms which are mirror image of each other. This will be explained shortly.

Some observations can be made about the tilings from Figure 2.2.5. Firstly, there is no one-to-one correspondence between the species of vertices and the types of tilings. Observe the species $3^3.4^2$ has two types of tilings ($3^3.4^2$) and ($3^2.4.3.4$).

Secondly, observe the tiling by the vertex type 4.6.12. The vertex type of this tiling can take 2 distinguishable orientations. Labeling a vertex in the clockwise direction results in a different notation from labeling the vertex in the anti-clockwise direction. For all the vertex types of the remaining tilings above, labeling the vertices in either direction makes no difference in the notation. Look at the tiling (4.6.12) in Figure 2.2.5. Fixing the notation of the vertex type to be labeled in a clockwise direction, the blue vertex is then 4.6.12 while the green one is 4.12.6. So if orientation is important, then neither tiling (4.6.12) nor tiling (4.12.6) can exist since both vertex types 4.6.12 and 4.12.6 are needed to form the desired Archimedean tiling. If we ignore orientation, then the tiling (4.6.12) exists.

Thirdly, notice that (3^4.6) has two kinds of tilings that are congruent to each other by a reflection. That is, one is an image of the other under a reflection. We say that these two tilings are *enantiomorphic*. Any figure without a line of symmetry and its image under a reflection or glide reflection are *enantiomorphs* of each other.

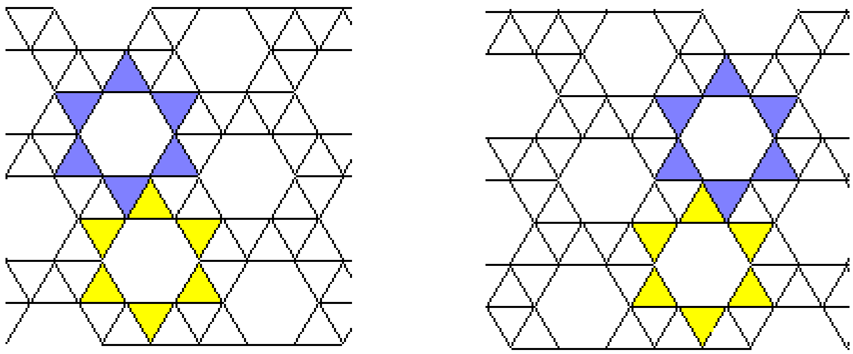

a   b

Fig 2.2.6 The two (3^4.6) tilings. In *a*, the topmost yellow triangle slides to the right of the bottom-most blue triangle. In *b*, the topmost yellow triangle slides to the left of the bottom-most blue triangle. Tiling *a* is known as the right-handed version while tiling *b* is known as the left-handed version.

Fourthly, observe the following tilings by vertex type 3^2.4.3.4. Suppose we colour the squares that are upright and their top and bottom triangles as shown below. It appears that the two tilings are different in the sense that Figure 2.2.7a is a right-handed version while Figure 2.2.7b is a left-handed version. Are these two tilings enantiomorphic?

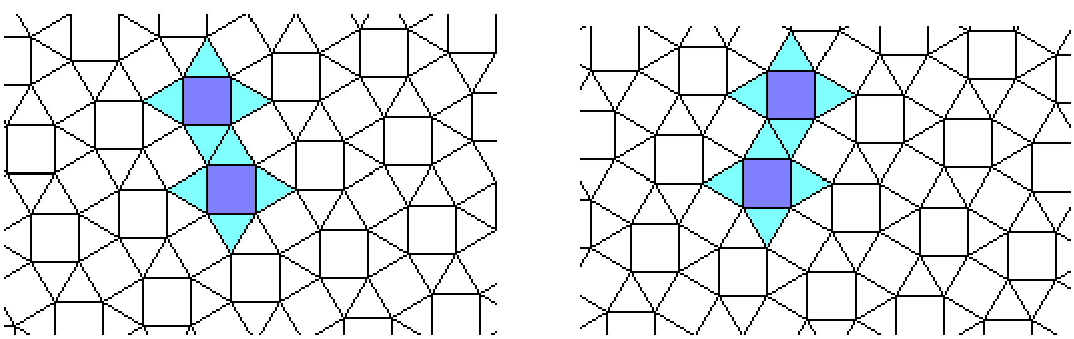

a   b

Fig 2.2.7 Tilings by vertex type 3^2.4.3.4

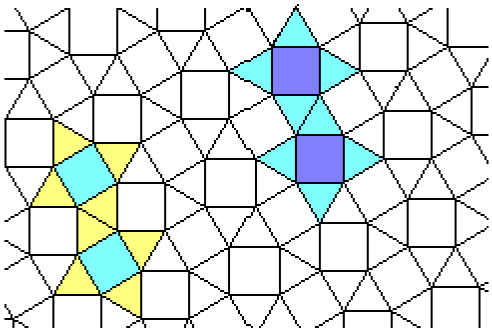

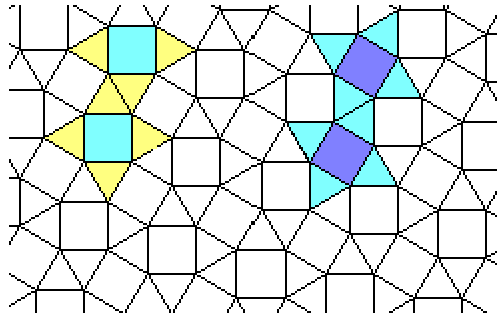

a b

Fig 2.2.8 Shading of the tilings by vertex type $3^2.4.3.4$

The two tilings are not enantiomorphic. Unlike the vertex type $3^4.6$ that has two kinds of tilings, the vertex type $3^2.4.3.4$ has only one tiling, that is, Figure 2.2.7a and Figure 2.2.7b are the same tiling. Look at Figure 2.2.8, which is a re-colouring of Figure 2.2.7. The new colouring shows that the tiling ($3^2.4.3.4$) has both the right versions and left versions. The green squares with yellow triangles form the left version while the blue squares with green triangles form the right version. In fact, Figure 2.28b is obtained by rotating Figure 2.2.8a. Rotating the two figures appropriately will lead to the tiling in Figure 2.2.1b. Using Figure 2.2.1b, it is easy to see the reflection symmetry in the tiling ($3^2.4.3.4$) as shown in Figure 2.2.9

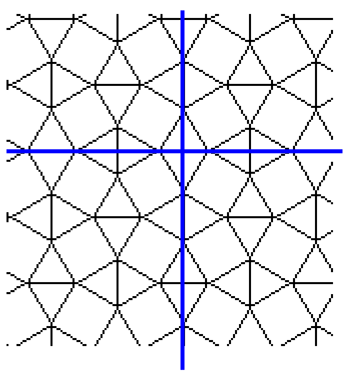

Fig 2.2.9 The reflection axes present in the tiling ($3^2.4.3.4$). They are shaded in blue.

($3^4.6$) is the only tiling of the eight Archimedean tilings that has no line of symmetry. We can conclude that up to congruency, each type of vertices gives rise to a unique tiling of the plane.

Finally, we say that a tiling is *vertex transitive* if given two vertices, there is a symmetry of the tiling that takes one onto the other. In a similar way, we can define a tiling that is *edge transitive* and a tiling that is *tile transitive*. We observe that Archimedean tilings are all vertex transitive and only 3.6.3.6 is edge-transitive. None of the Archimedean tilings are tile transitive but all the Platonic tilings are tile transitive.

2.3 Tilings and Their Wallpaper Symmetry Groups

Let us now classify the eleven tilings into the wallpaper symmetry groups. The analysis is provided in the table below. The analysis is done with Chart 1.6.2 on page 22.

Tiling	Figure	Symmetry Axes, Rotation centers and Primitive cells	Symmetry Group
(3^6)	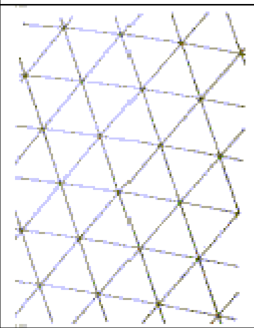	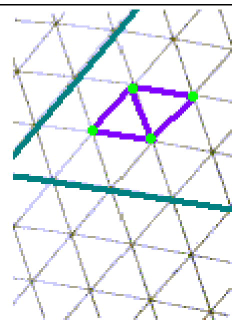	p6m
(4^4)	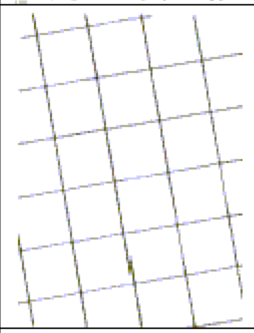		p4m
(6^3)	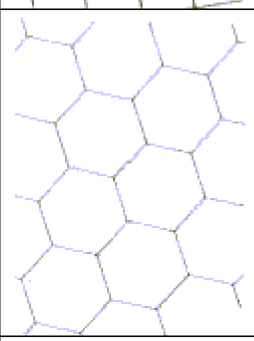	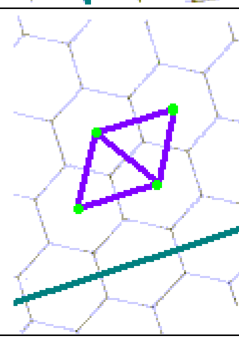	p6m
$(3^4.6)$	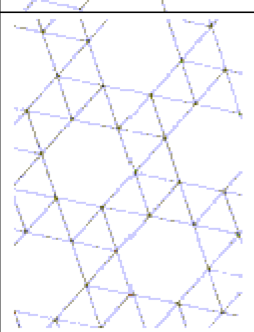	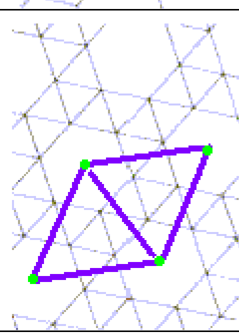	p6

Tiling	Figure	Symmetry Axes, Rotation centers and Primitive cells	Symmetry Group
$(3^3.4^2)$	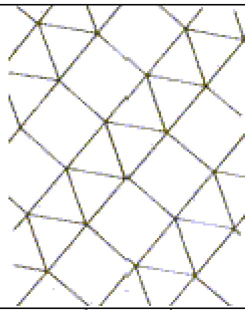	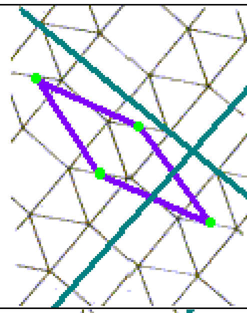	cmm
$(3^2.4.3.4)$	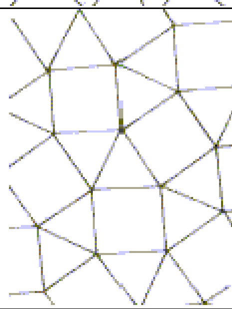	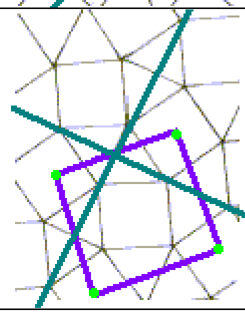	p4g
(3.4.6.4)	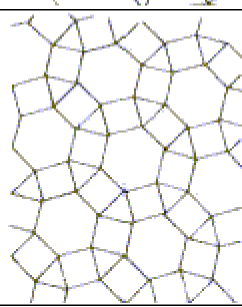	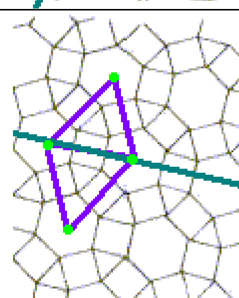	p6m
(3.6.3.6)	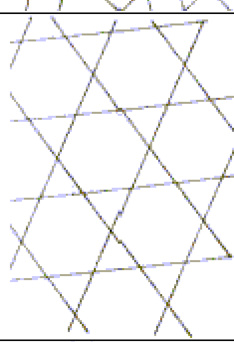	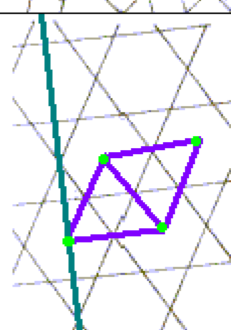	p6m
(3.12^2)	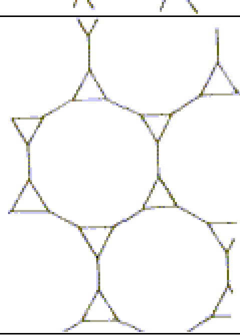	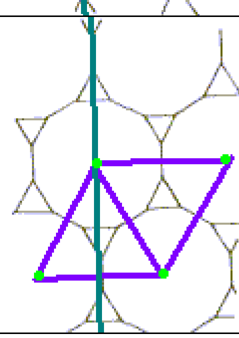	p6m

Tiling	Figure	Symmetry Axes, Rotation centers and Primitive cells	Symmetry Group
(4.6.12)	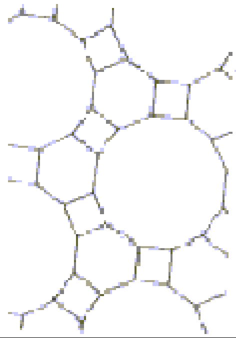	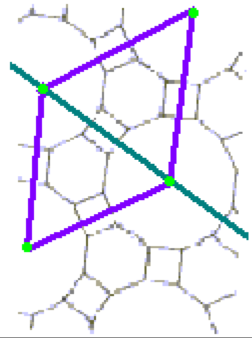	p6m
(4.8^2)	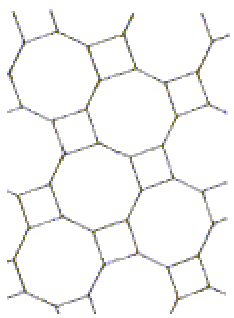	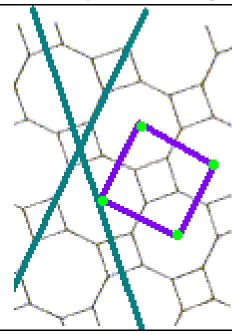	p4m

Table 2.3.1

To summarise this section, there are only 5 different wallpaper groups into which the Platonic and Archimedean tilings can be classified into, namely *p6*, *p6m*, p4g, *p4m* and *cmm*. I recommend the following checklist to identify the correct symmetry group for each of the eleven tilings.

1) For a tiling with six as the highest order of rotation,
    a) if it admits reflection, it belongs to the group *p6m*.
    b) Otherwise, it belongs to *p6*.

3) For a tiling with four as highest rotation order,
    a) if it has triangular tiles, it belongs to *p4g*.
    b) Otherwise, it belongs to *p4m*.

4) A tiling with only rotation of order two has to be a *cmm* pattern.

Chapter 3

Fractals

3.1 Introduction

An object has *self-similarity* if parts of the object look similar to the whole object under any magnification. A *fractal* is an object or figure that exhibits self-similarity. We shall now look at a fractal called the *Koch curve* and by understanding its construction, we will see why the Koch curve exhibits self-similarity.

Let us start constructing the Koch curve now. We begin with a straight line. We remove the middle third of the straight line and replace it with the top of an equilateral triangle.

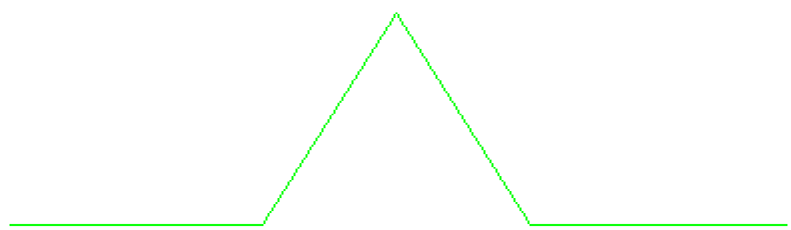

Fig 3.1.1 First step in the making of the Koch Curve

Now, for every straight line segment in the figure, we replace its middle third with the top of an equilateral triangle. The following figures show the subsequent steps in the making of the Koch curve.

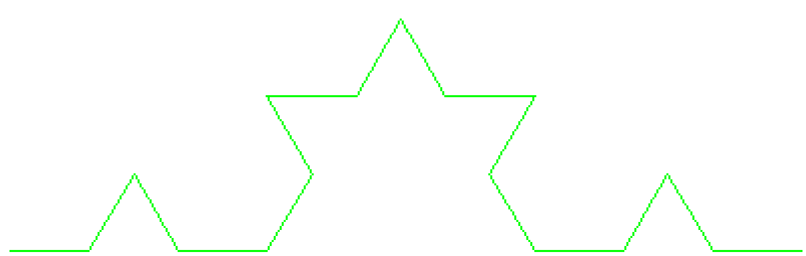

a) Second step

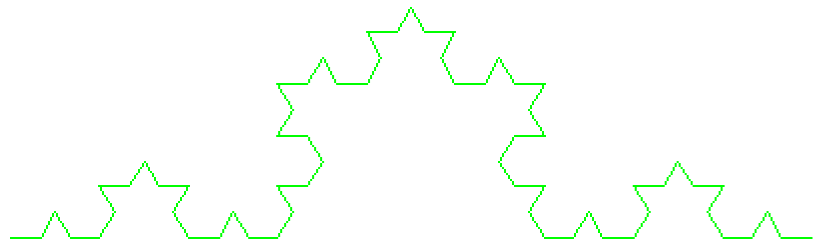

b) Third step

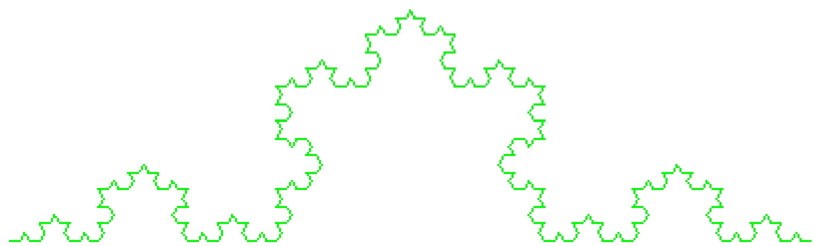

b) Forth step

Fig 3.1.2 Steps in the making of the Koch curve

As we carry on building the Koch curve, the figure changes a little and the changes are not obvious to the naked eye. It is not possible to present a perfect Koch curve, since by construction, the Koch curve is achieved by implementing infinite steps. However, we can present a rendering of the Koch curve, which looks close to the perfect Koch curve. With our naked eyes, we cannot tell the difference between a rendering of the Koch curve and a perfect Koch curve.

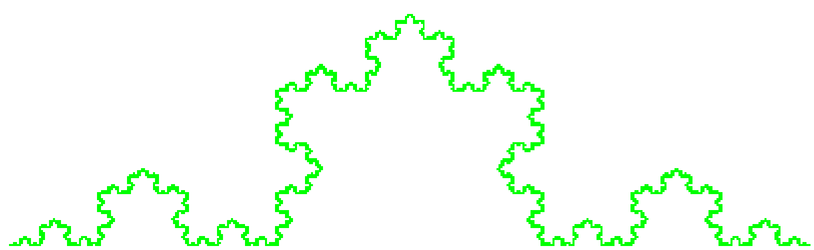

Fig 3.1.3 A rendering of the Koch curve

The Koch curve can be re-produced by a *recursive process*, in which the same set of rules is applied over and over with the end product at each step becoming the starting point for the next step. The recursive process of producing the Koch curve can be described as below:

1) Begin with a straight line.
2) Remove the middle third of every straight line segment and replace with the top of an equilateral triangle.

By the above construction of the Koch curve, it is easy to see that the Koch curve exhibits self-similarity. In fact, it exhibits *exact self-similarity*. Every magnification of any part of the curve will look exactly like the whole curve.

3.2 Dimension of the Koch Curve

Let us now calculate the length of the Koch curve. Suppose we begin with a straight line of length L. Let L_n denote the length of the Koch curve after the *n*th step. After the first step, the number of straight line segments is 4 and each has a length of $^1/_3$L. So $L_1 = {}^4/_3L$. After the second step, the number of straight line segments is 4^2 and each has a length of $(^1/_3)\ (^1/_3L) = (^1/_3)^2L$. This gives us $L_2 = (^4/_3)^2\ L$. Counting in this manner, after the *n*th step, we get 4^n straight line segments of length $(^1/_3)^nL$ each. Hence, $L_n = (^4/_3)^n\ L$. Taking *n* to the infinity, we see that the length of the Koch curve is infinite.

We proceed to determine the *fractal dimension*, *D*, the extent of the wiggliness, of the Koch curve. The closer *D* is to the value one, the less wiggly it is. The following equation gives the fractal dimension.

$$L = C\ .\ l^{1-D} \quad (3.1$$

L = length of the fractal curve
l = length of measuring stick
D = fractal dimension
C = constant that is a certain measure of apparent length

Let us take measuring sticks of length $(^1/_3)^n$ and $(^1/_3)^m$ for some n, m ϵ IN – {0}. Then we solve the following system of equations:

$$(^4/_3)^n = C\ .\ (^1/_3)^{n\ (1-D)} \quad (3.2)$$

$$(^4/_3)^m = C\ .\ (^1/_3)^{m\ (1-D)} \quad (3.3)$$

Dividing Equation 3.2 by Equation 3.3, we get

$$(^4/_3)^{n-m} = (^1/_3)^{(n-m)\ (1-D)} \quad (3.4)$$

Taking logarithm on both sides of Equation (3.4), we get D = 1.26.

3.3 The Sierpinski Triangle

Another fractal with exact self-similarity is the *Sierpinski triangle*. Like the Koch curve, the Sierpinski triangle is reproduced by a recursive process. The recursive process in producing the Sierpinski triangle is as follows.

We begin with any solid triangle *ABC*. We mark the midpoints of *AB*, *BC* and *AC* as *M*, *N* and *P* respectively. Remove the triangle *MNP*. Call *MNP* the *middle triangle* of *ABC*.

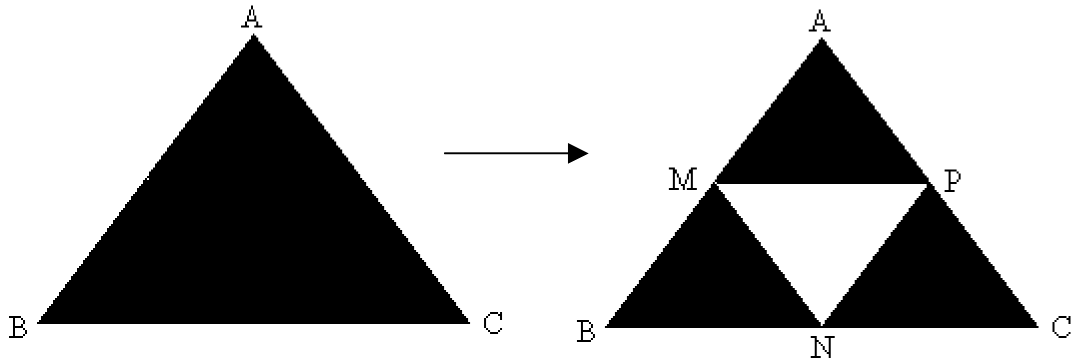

Fig 3.3.1 First step in the making of the Sierpinski traingle

We now have three solid triangles *AMP*, *MBN* and *PNC*. Again, we mark the midpoint of the edges of each of these triangles and remove the middle triangle of each of the three solid triangles. We will get the following figure.

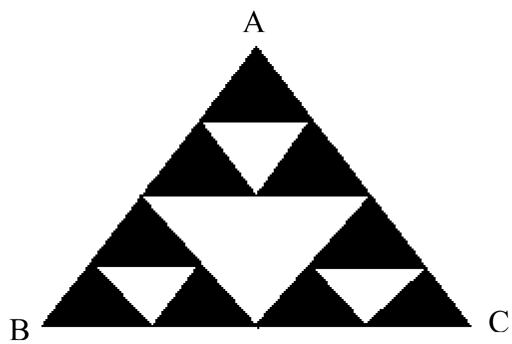

Fig 3.3.2 Second step in the making of the Sierpinski triangle

To get the Sierpinski triangle, we repeatedly remove the middle triangles of all solid triangles that are obtained after each step. The following figure shows a rendering of the Sierpinski triangle. We can see that the perfect Sierpinski triangle which is obtained after infinite steps has exact self-similarity.

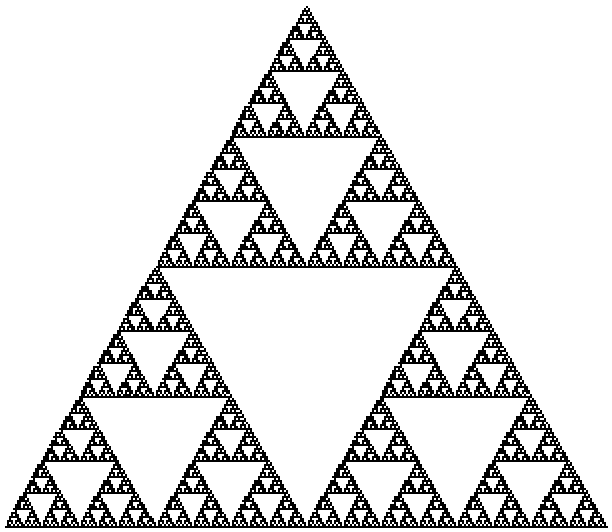

Fig 3.3.3 A rendering of the Sierpinski triangle

The recursive process of producing the Sierpinski triangle can be described as below:

1) Begin with a solid triangle.
2) Remove the middle triangle of every solid triangle.

3.4 Approximate Self-similarity

The Sierpinski triangle and the Koch curve are examples of fractals that have exact self-similarity. This means that magnification of any part of the fractal will resemble the whole fractal. However, some fractals only have *approximate self-similarity*, that is, we do not see exactly the same things on every magnification, but there exists some resemblance to the original object at each magnification. Examples of objects that have approximate self-similarity are mountains, trees and coastlines. Most natural objects have this property of approximate self-similarity. Physical objects are considered to be fractals if they have approximate self-similarity over a range of magnifications in which the largest is at least ten times the smallest.

Look at the following pictures of a cauliflower. Figure 3.4.1b is a close-up of the part enclosed by the white square in Figure 3.4.1a. Observe that the cauliflower displays approximate self-similarity, since the close up image appears like another cauliflower head, but somewhat unlike the original one.

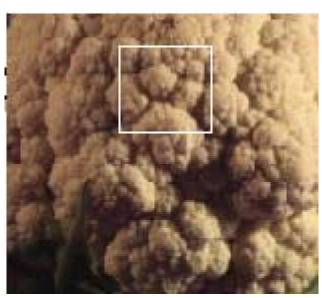

a

Fig 3.4.1 Pictures of a cauliflower head.

Coastlines exhibit approximate self-similarity. They have about the same amount of wiggliness on most magnifications. When viewed on a large scale, the wiggliness is caused by global features such as inlets. When viewed on a small scale, the wiggliness is caused by local features such as big rocks. Let us measure the extent of the wiggliness of one particular coastline, the coastline of Great Britain.

Fig 3.4.2 Coastline of Great Britain

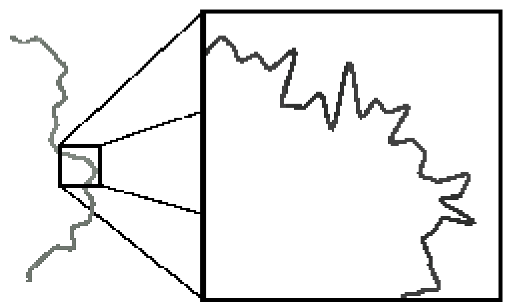

Figure 3.4.3 Magnification of part of a coastline

To determine the extent of wiggliness, that is, the fractal dimension of the coastline, we need to find out the length of the coastline on the map. To do so, we line measuring sticks along the coastline on the map and calculate the total length of the sticks. According to figures adapted from Davis **[10]**, with sticks of 0.5 inches long, 15.9 rods are needed, thus an approximate length of the coastline is 7.95 inches. With sticks of length $^3/_{32}$ inches, 141 rods are needed, giving an approximate length of 13.2 inches. The shorter the sticks, the longer the estimation is. In fact, the approximations grow arbitrarily large as the sticks become shorter.

a

Fig 3.4.4 Lining the coastline with measuring sticks of different lengths

Using Equation (3.1) and the two approximations of the coastline, we get the following system of equations:

$$7.95 = C\ (0.5)^{1-D} \tag{3.5}$$

$$13.2 = C\ (^{3}/_{32})^{1-D} \tag{3.6}$$

Dividing Equation 3.4 by Equation 3.5, we get

$$7.95/13.2 = (^{0.5}/\ _{3/32})^{1-D} \tag{3.7}$$

Taking logarithm on both sides of Equation (3.7), we get D = 1.3.

To get a feel of what D = 1.3 implies, a straight line segment has D = 1 and the Koch curve, which is wiggly, has D = 1.26. So the coastline is even wigglier than the Koch curve!

3.5 Applications of Fractals

Fractals are used to simulate images of natural landscape. Hence, fractals are particularly useful in science-fiction movies in creating realistic-looking landscape. For example, to get a mountainous landscape, we construct a variation of the Sierpinski triangle as follow:

1) Start with any solid triangle ABC.
2) Remove the middle triangle of every solid triangle.
3) For each removed triangle, move its vertices in a random direction by a small magnitude in relation to the length of corresponding side of the solid triangle, say 25% of the length.
4) Go to (2).

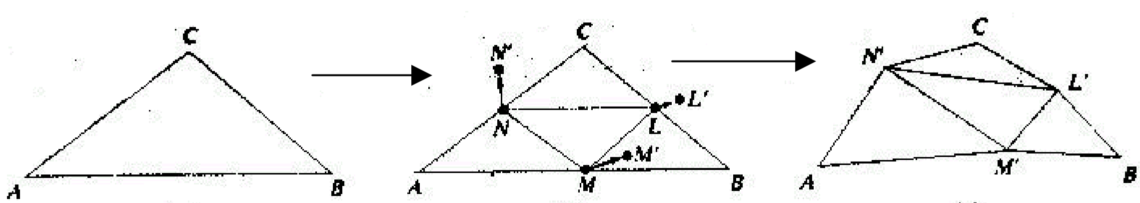

Fig 3.5.1 Moving the vertices of the middle triangle by a small magnitude in relation to the length of the corresponding side of the triangle ABC.

Fig 3.5.2 The first two steps in creating a mountain look

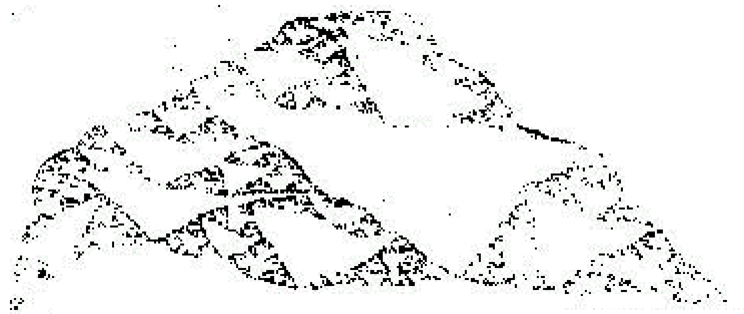

Fig 3.5.3 A mountainous landscape which resulted after some *n* steps

An *affine transformation* is a method of transforming figures in space by rotation, stretching, reflecting and translating. It is of the form f(x,y) = (ax + by + c, mx + ny + q), a, b , c, m, n, q ϵ IR. Due to the self-similarity property of fractals, smaller versions of a fractal can be obtained by rotating, stretching or reflecting, combined with translating, the original big version of the fractal. Hence, a fractal image can be described completely by a set of affine transformations. This special property of fractals leads to an application of fractals known as the fractal image compression. *Fractal image compression* is a technique to store an image by storing its affine transformations instead of storing the image itself. Storage affine transformations comparatively reduces the computer space utilized since affine transformations involve only numbers, unlike the actual image, which has a lot of details such as colouring. The fractal fern in Figure 3.5.4 is completely described by the following affine transformations with their respective probabilities *p*. The probabilities of the affine transformations affect the colouring of the fractal image. The set of affine transformations of a fractal is known as the *iterated function system* of the fractal.

$f_1(x,y) = (0.00, 0.16y)$ with $p = 0.01$
$f_2(x,y) = (0.85x + 0.04y, -0.04x + 0.85 + 1.6)$ with $p = 0.85$
$f_3(x,y) = (0.2x - 0.26y, 0.23x + 0.22y + 1.6)$ with $p = 0.07$
$f_4(x,y) = (-0.15x + 0.28y, 0.26x + 0.24y + 0.44)$ with $p = 0.07$

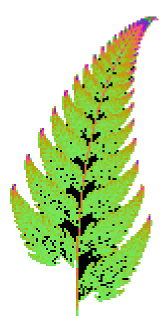

Fig 3.5.4 A fractal fern generated on a software, *Fractal Explorer*

3.6 Symmetric Fractals – Finite Designs Revisited

Using the idea of the iterated function system, we can produce pictures of symmetric fractals. A *symmetric fractal* is a finite design that is created by an affine transformation and elements from the symmetry group of the fractal. Recall that finite designs are bounded figures and they belong to either the cyclic symmetry group or the dihedral symmetry group.

Below are some examples of symmetric fractals that are generated by affine transformations on a software, *Fractal Explorer*. Please refer to Appendix I to see the iterated function system for each of the following symmetric fractals.

Symmetric Fractal	Name of Fractal	Symmetry Group
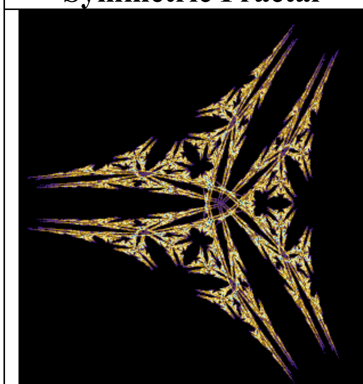	Bee	D_3
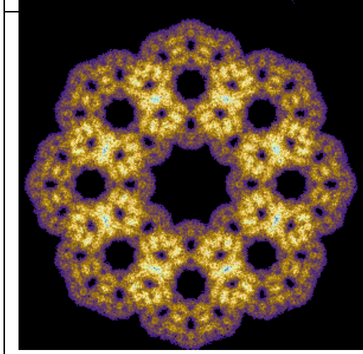	Doily	D_8
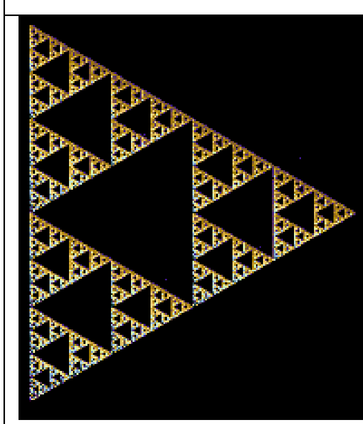	Sierpinski Triangle	D_3

Symmetric Fractal	Name of Fractal	Symmetry Group
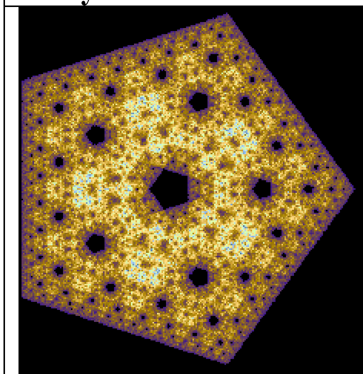	Sierpinski Pentagon	D_5
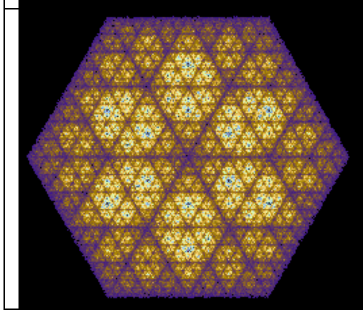	Sierpinski Hexagon	D_6

Table 3.6.1

Chapter 4

Kaleidoscopes

4.1 Introduction

A kaleidoscope is a mirror system that creates aesthetically pleasing designs by reflection. Look at the following figures. The figures shown in Figure 4.1.1 below are created by a 2-mirror kaleidoscope.

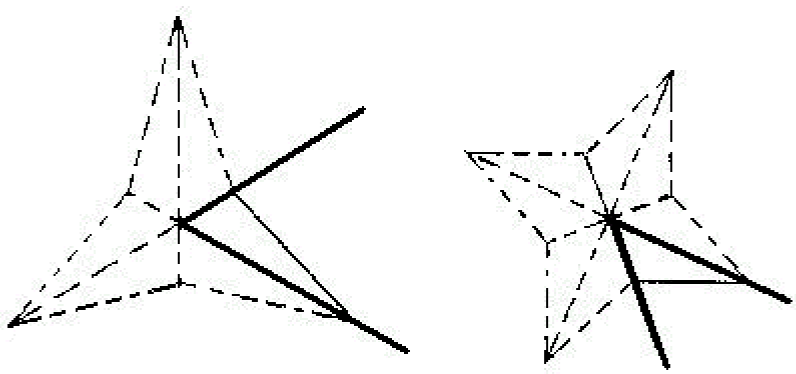

a *b*

Fig 4.1.1 Two figures which are created by two mirrors. The mirrors are represented by the bold lines and the dotted parts of the figures are reflections of the basic designs. The basic design for each figure is shown in Fig 4.1.2.

It is advisable to have some plane mirrors to play around with as we explore kaleidoscopes. Some figures will be presented and it is fun to use mirrors to check out their images and see the overall design. In our context, the *overall design* refers to the figure consisting of the original design and its reflections in the mirrors. It is created by placing our mirrors perpendicular to the plane of the basic design. The overall designs in Figure 4.1.1 are created by using the figures in Figure 4.1.2 as basic designs.

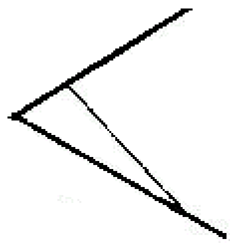

a

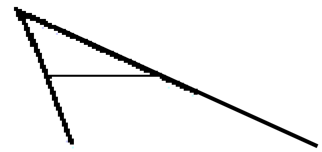

b

Fig 4.1.2 The basic designs used in creating Fig 4.1.1, with the mirrors in bold.

Look at Figure 4.1.3. Place the mirrors as shown in the figure. Look into mirror with your sightline close to mirror 1. Now, look into mirror 2 with your sightline close to mirror 2. Shift your sightline slowly from mirror 2 back to mirror 1. What do you observe?

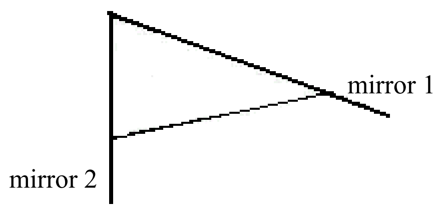

Fig 4.1.3

The overall design created by Figure 4.1.3 does not look as "pleasing" as those in Figure 4.1.1. Looking into mirror 1 and looking into mirror 2 give different overall designs, as shown in Figure 4.1.4. As the sightline shifts from mirror 1 to mirror 2, different overall designs occur. Observe that Figure 4.1.2 gives the same overall design regardless of the position of the sightline unlike Figure 4.1.3. So we say that the overall design for Figure 4.1.3 is *ambiguous* and not pleasing while the ones for Figure 4.1.2 are *unambiguous* and pleasing.

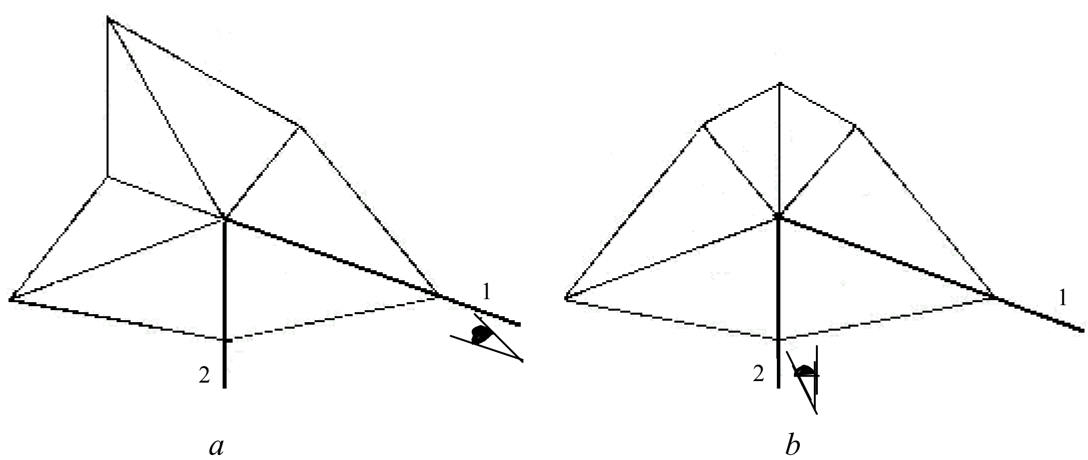

Fig 4.1.4

Fig 4.1.4a shows the overall design when we look into mirror 1 with the sightline close to mirror 1.
Fig 4.1.4b shows the overall design when we look into mirror 2 with the sightline close to mirror 2.

The above experiment makes us realise that some angles between the mirrors give pleasant overall designs while some do not. We will call those angles that give unambiguous overall designs *good kaleidoscope angles*. Otherwise, they are known as *bad kaleidoscope angles*.

In this chapter, we will look into 2-mirror kaleidoscopes and 3-mirror kaleidoscopes. We will investigate what are good and bad kaleidoscope angles.

4.2 Two-mirror Kaleidoscopes

How the 2-Mirror Kaleidoscope Works

To simplify our discussion, we will use triangular wedges as our basic design. Using such wedges help us to see what kinds of angles are good kaleidoscope angles and what kinds are bad.

Consider the following wedge with the mirrors at an angle of $\pi/5$ away from each other. Place the mirrors as shown in the diagram and observe the images in the mirror. The overall design should be a five-pointed star as shown in Figure 4.2.2.

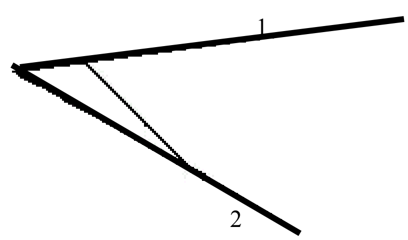

Fig 4.2.1 Wedge with mirrors at angle $\pi/5$

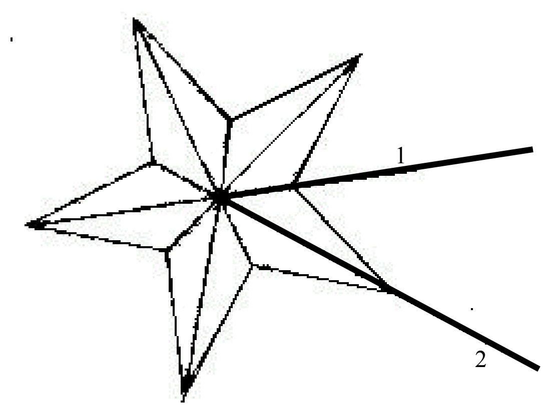

Fig 4.2.2 The overall design with Fig 4.2.1 as the basic design

Let us see how a five-point star is created by Figure 4.2.1. Call the original wedge *W* and dissect the overall design into regions as shown in Figure 4.2.3. The region *S*, which is behind the two mirrors, is known as the *shadow*. Note that each region contains either a direct copy or reverse copy of *W*. Name the image in each region as R_m, as shown in the following list, where *R* denotes the region from which the image is mapped and *m* denotes the mirror axis concerned. We proceed to explain how the list is obtained.

Image in A = W_2
Image in B = W_1
Image in C = B_2
Image in D = A_1
Image in E = D_2
Image in F = C_1
Image in G = F_2
Image in H = E_1
Image in S = G_1 and H_2

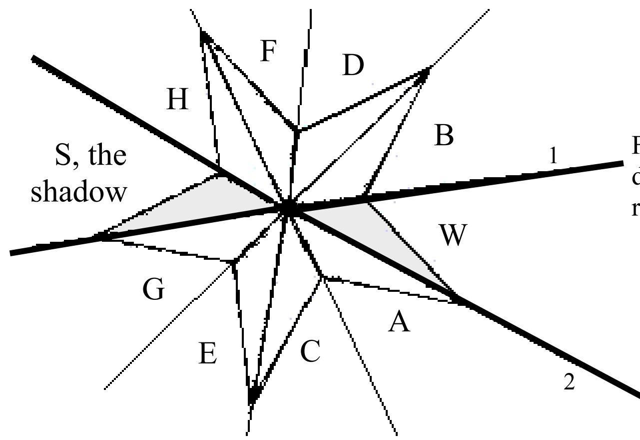

Fig 4.2.3 The overall design dissected into regions

Firstly, the image in A is obtained by simply flipping over *W* in the mirror line 2. Similarly, the image in B is obtained by flipping over *W* in the mirror line 1.

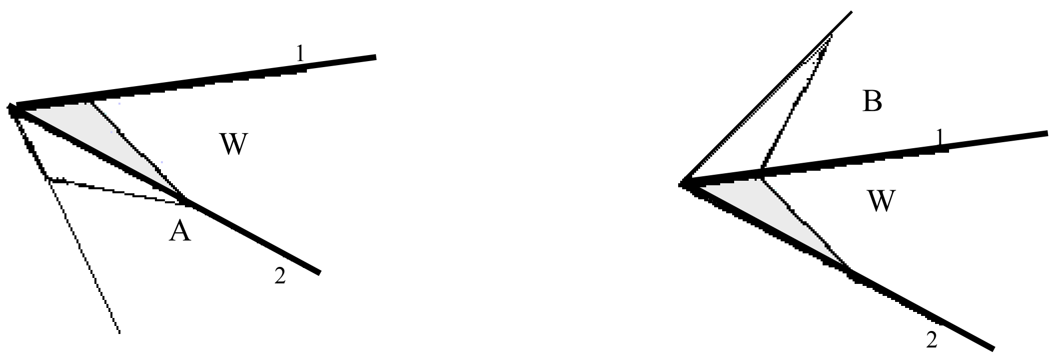

Fig 4.2.4 Image in A is obtained by flipping over W in 2. Image in B is obtained by flipping over W in 1.

To see how C is obtained by reflection, we choose two points P_1 and P_2 which are close to the vertices of the wedge in C and determine from where P_1 and P_2 are mapped. A schematic diagram is shown in Figure 4.2.5. Points P_1 and P_2 are shown as blue dots. Let us consider point P_1. We draw a line from P_1 to the eye. This line is known as the *line of reflection* and it is of angle θ from the normal of mirror 2. Let the line of reflection meet the mirror axis at *M*. Determine the distance MP_1. We draw a line MP_1'of length MP_1 and at an angle θ from the normal at M. This line is known as the *line of incidence*. The endpoint of this line, P_1', is the point from which P_1 is mapped. Similarly, we can determine from where P_2 is reflected. The points from which P_1 and P_2 are reflected are shown as green dots in the diagram and labelled P_1'and P_2' respectively.

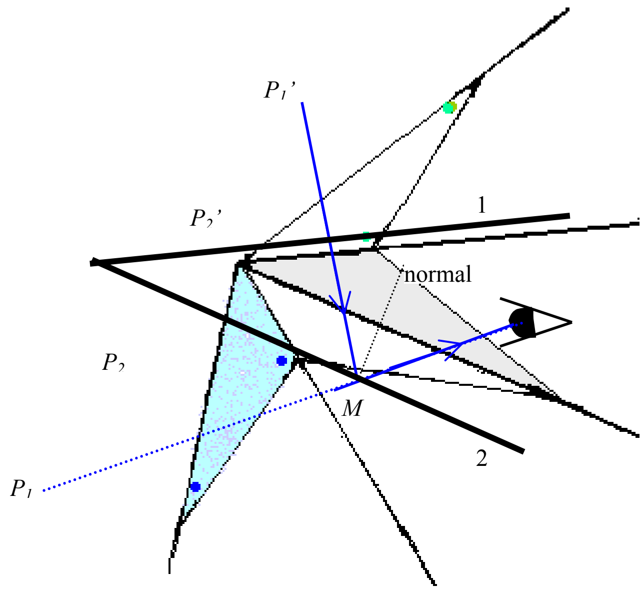

Fig 4.2.5 A schematic diagram, not drawn to scale, to show from where point P_1 is reflected. The image in C is shaded light green while the original wedge is shaded grey.

Both the points P_1'and P_2' fall inside the region B. If we repeat the procedure for all the points in C, we will realise that all these points are mapped from points in B. However, in this case, it is sufficient to consider only the two points P_1 and P_2. Hence, C is a reflection of B in mirror 2. Similarly, we can determine from where the other regions, except the region *S*, are mapped. Let us now see from where the image in *S* is mapped.

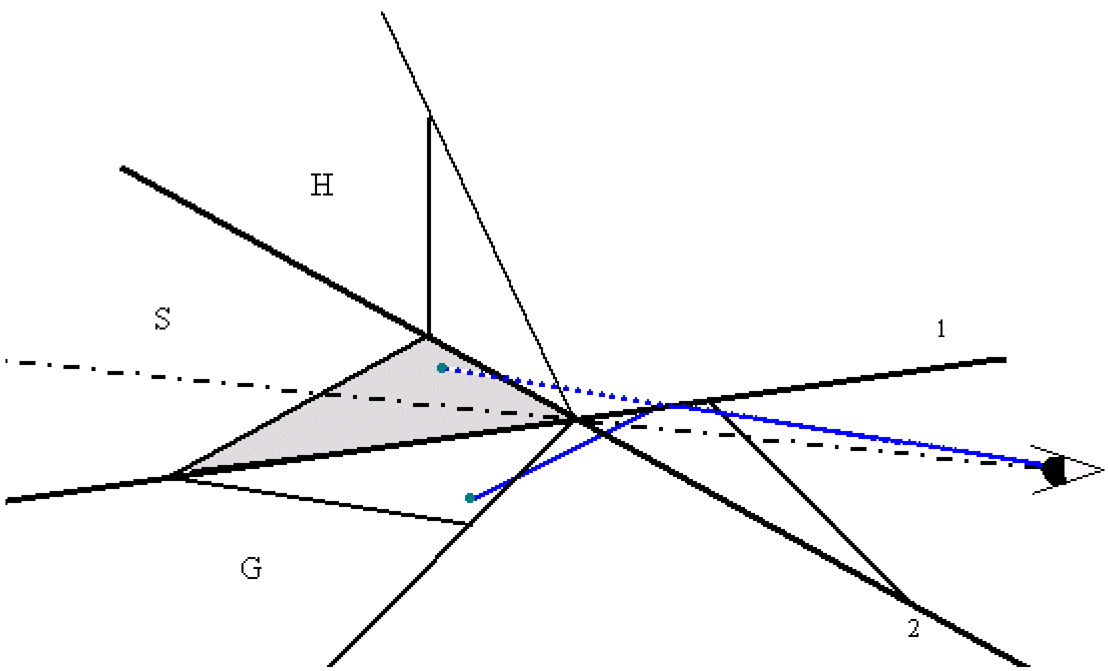

Fig 4.2.6 The black dashed axis from the eye to the intersection of the mirrors cuts the shadow region into 2 regions. Consider a point from the top part of the shadow. As shown above, it is reflected from a point in region G in mirror 1.

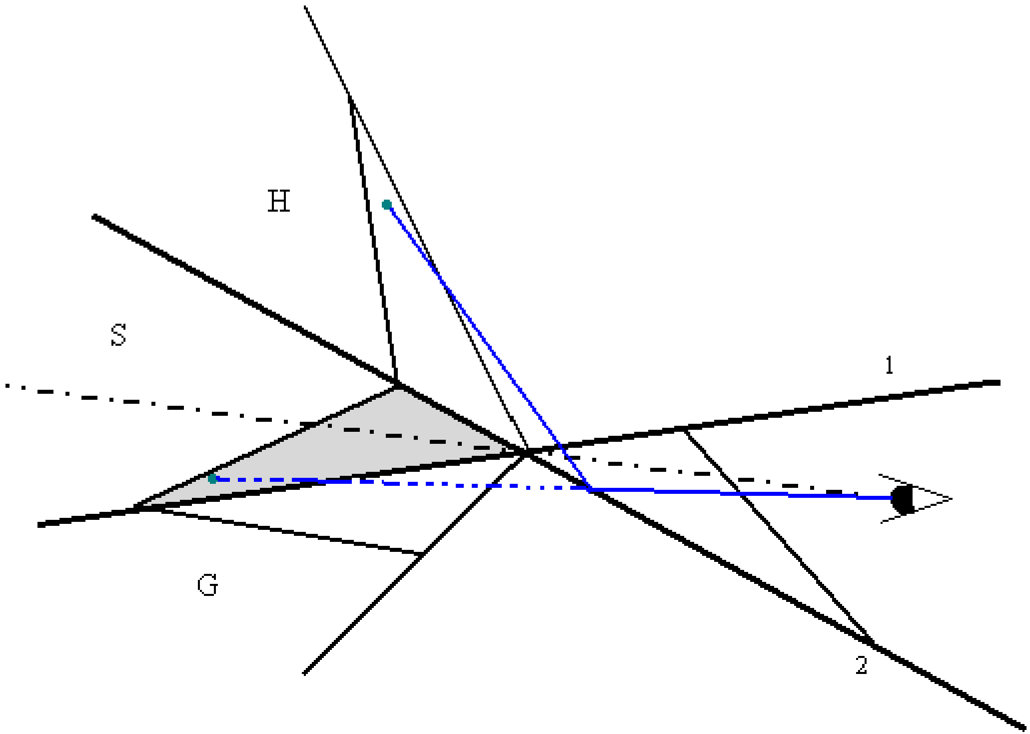

Fig 4.2.7 Consider a point from the bottom part of the shadow. As shown above, it is reflected from a point in region *H* in mirror 2.

From Figures 4.2.6 and 4.2.7, we see that the image in S is mapped from G and H. Its top image is mapped from G in mirror 1 and its bottom part is mapped from H in mirror 2.

Getting Good Kaleidoscope Angles

Try the following experiment as shown in Figure 4.2.3. Using the given green straight line as our basic design and a fixed mirror axis where you place the mirror, pivot your second mirror about the blue dot. Turning the second mirror about the pivot gives us different mirror angles. Observe the overall designs with each different angle you try.

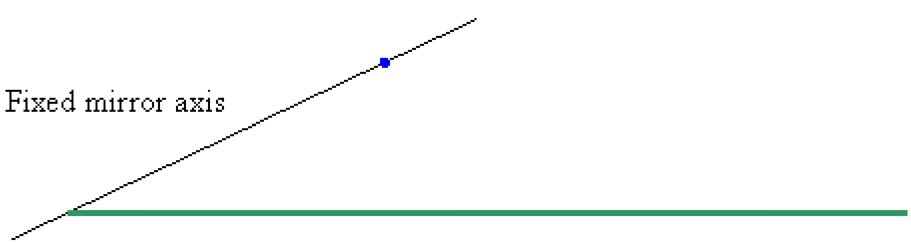

Fig 4.2.3 Experiment to observe the overall designs with different angles

Experimenting with different angles between mirrors, we observe that some angles give n-pointed stars, for some natural number n, while some do not. We shall try to find the angles that create n-pointed stars and such angles shall be our *good kaleidoscope angles*.

Suppose we start with a good kaleidoscope angle θ and we get a n-pointed star for some natural number n. To get a n-pointed star, we need $2n$ copies of the original wedge W, n

copies which are reverse copies of W and n copies which are direct copies, including W itself. To have $2n$ copies of the original around the vertex where the two mirrors meet would necessarily imply that $\theta = {}^{2\pi}/_{2n}$, ie $\theta = {}^{\pi}/_{n}$. So, a good kaleidoscope has to be in the form $\theta = {}^{\pi}/_{n}$.

Now, we need to check whether $\theta = {}^{\pi}/_{n}$ is a good kaleidoscope angle for all natural number $n > 1$. Now, the angle around a vertex is 2π. The number of copies of W around the vertex is therefore ${}^{2\pi}/_{\theta} = 2n$. We lay down copies of W edge-to-edge around the vertex where the mirrors meet. The copies alternate between a reverse copy and a direct copy of W. So there are n pairs of a direct copy and a reverse copy, thus forming a n-pointed star.

With the above argument, we establish that an angle θ is a good kaleidoscope angle if and only if $\theta = {}^{\pi}/_{n}$ for n >1. Notice that a good kaleidoscope angle is at most a right angle.

4.3 Three-mirror Kaleidoscopes

We are interested in triangular kaleidoscopes that are formed by three plane mirrors placed perpendicularly to the plane of the basic design. Here, we will find the good kaleidoscope angles of three-mirror kaleidoscopes. For a start, observe the overall designs of Figure 4.3.1.

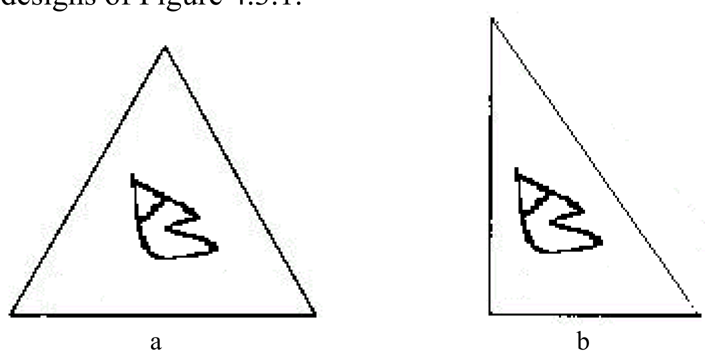

Fig 4.3.1 Place the mirrors along the edge of the above triangles to view the overall designs of *a* and *b*.

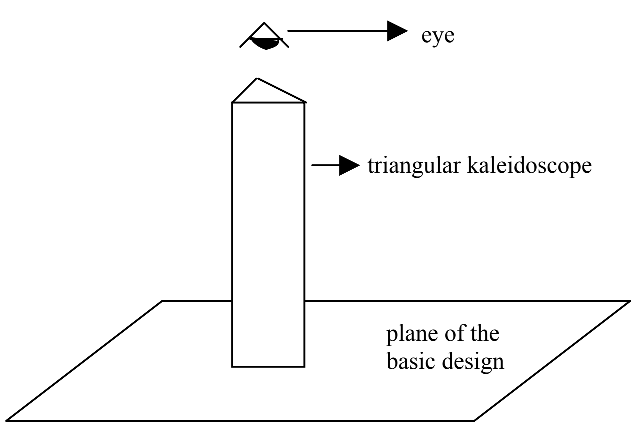

Fig 4.3.2 The correct way of viewing the overall design

Figure 4.3.1a shows a kaleidoscope configuration with an unambiguous overall design while Figure 4.3.1b shows one that gives an ambiguous overall design. In a three-mirror kaleidoscope, there are three places where two mirrors meet. To be a good kaleidoscope, it is essential that each angle of intersection of the mirrors is a good kaleidoscope angle. Each angle must be of the form π/n for some natural number $n > 1$. Now, we want to find out precisely what are the angles that qualify as good kaleidoscope angles for a three-mirror kaleidoscope.

Consider the triangle *ABC*, which is the base of our kaleidoscope. Let the angles in *ABC* be π/n, π/m and π/p for some $n, m, p \in \mathbb{N} - \{0, 1\}$. Let us fix $n \leq m \leq p$. The sum of the angles must be π.

So, $$\pi/n + \pi/m + \pi/p = \pi \qquad (4.1)$$

Giving us $$1/n + 1/m + 1/p = 1 \qquad (4.2)$$

<u>Case 1: n = 2</u>

Equation (4.2) gives us $$1/m + 1/p = 1/2 \qquad (4.3)$$

m cannot take the value of 2, else $1/p = 0$.

If m = 3, then (4.3) becomes $1/3 + 1/p = 1/2$, giving us $1/p = 1/6$.

If m = 4, then $1/p = 1/4$.

If $m \geq 5$, then $p < m$, which is not what we want, since we have fixed $n \leq m \leq p$.

Thus, if n = 2, we have two sets of solutions to (4.3), namely

1) n = 2, m = 3, p = 6
2) n = 2, m = 4, p = 4

<u>Case 2: n = 3</u>

Equation (4.2) gives us $$1/m + 1/p = 2/3 \qquad (4.4)$$

If m = 3, then p = 3. If $m \geq 4$, then $p < m$, which is not what we want.

Thus, if n = 3, we have a set of solutions to (4.4), namely:

n = 3, m = 3, p = 3

Case 3: $n \geq 4$

Then, $m \geq 4$ and $p \geq 4$.

ie $\quad {}^1/_m \leq {}^1/_4$ and ${}^1/_p \leq {}^1/_4$

ie $\quad {}^1/_n + {}^1/_m + {}^1/_p \leq {}^3/_4$, which is not what we want.

Hence, we have obtained all possible sets of good kaleidoscope angles, namely

1) ${}^\pi/_3, {}^\pi/_3, {}^\pi/_3$
2) ${}^\pi/_2, {}^\pi/_4$ and ${}^\pi/_4$
3) ${}^\pi/_2, {}^\pi/_3$ and ${}^\pi/_6$

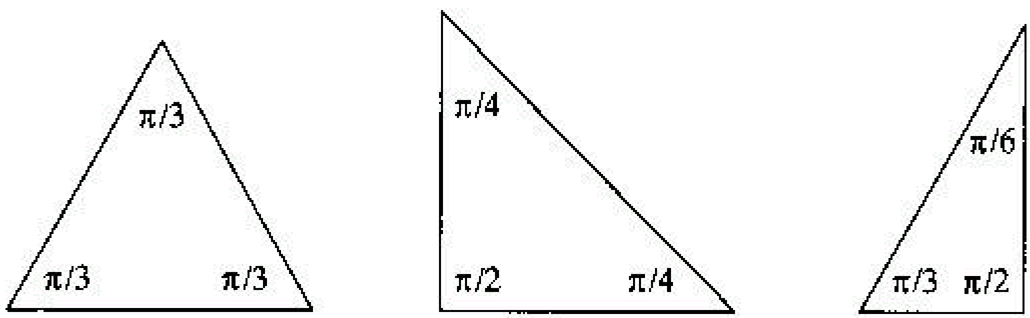

Fig 4.3.3 The configurations for good three-mirror kaleidoscopes

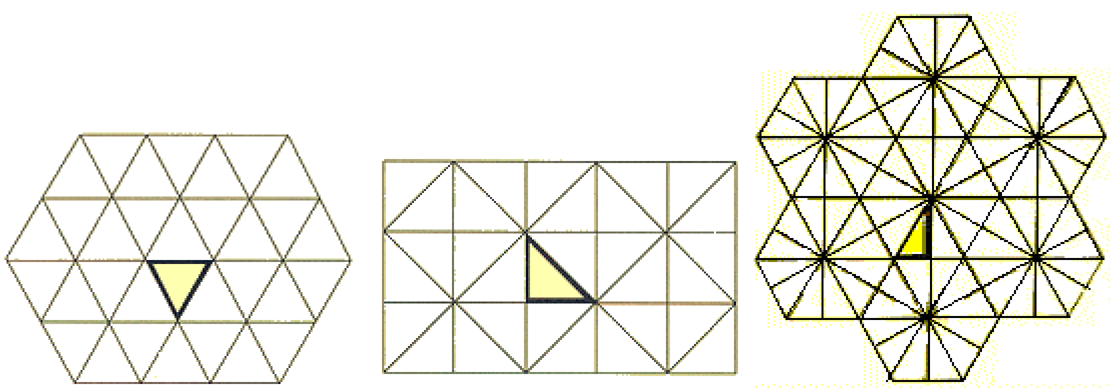

Fig 4.3.4 The corresponding overall designs for the (${}^\pi/_3, {}^\pi/_3, {}^\pi/_3$), (${}^\pi/_2, {}^\pi/_4, {}^\pi/_4$) and (${}^\pi/_2, {}^\pi/_3, {}^\pi/_6$) kaleidoscopes configuration with the shaded regions as the basic design.

There are two differences between the two-mirror kaleidoscopes and our three-mirror kaleidoscopes. Firstly, the two mirror kaleidoscopes involve an infinite region as the basic design while our three-mirror ones involve a finite region. Secondly, the two-mirror ones generate a finite cell while our three-mirror ones generate infinite cells as an overall design. The infinite cells generate a tiling-like overall design.

Readers who are interested in building their own two-mirror or three mirror kaleidoscopes can refer to Gay **[23]**, page 211 to 216.

Chapter 5

The Golden Ratio

5.1 Introduction

Suppose we want to divide a line AB at C such that AC is longer than BC and the ratio of AC to BC is equal to the ratio of AB to AC. We will determine the value of this common ratio $\mu = \frac{AC}{BC} = \frac{AB}{AC}$.

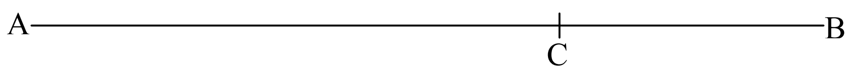

Fig 5.1.1

Let AB = a and so, AC = ${}^{a}/_{\mu}$.

Since $\frac{AC}{BC} = \frac{AB}{AC}$, therefore $(AC)^2 = AB\,(BC)$

$$\Rightarrow \quad ({}^{a}/_{\mu})^2 = a\,(a - AC)$$

$$\Rightarrow \quad ({}^{a}/_{\mu})^2 = a\,(a - {}^{a}/_{\mu})$$

$$\Rightarrow \quad ({}^{1}/_{\mu})^2 = 1 - {}^{1}/_{\mu}$$

$$\Rightarrow \quad \mu = 1 + {}^{1}/_{\mu} \qquad (5.1)$$

$$\Rightarrow \quad \mu^2 = \mu + 1 \qquad (5.2)$$

Considering only the positive solution to Equation (5.2), $\mu = {}^{(1 + \sqrt{5})}/_{2} = 1.618\ldots.$
This value of μ is known as the *golden ratio*. It is also known as the *golden section* or the *divine ratio*.

Conversely, given any line segment AB, we may want to extend it to a line AE such that $\frac{AE}{AB} = \mu$. We will now explain how to construct this extension geometrically. Given any line AB of length a, construct a square ABCD. Bisect AB and let the midpoint be M. With M as a center, draw an arc with radius MC to cut AB produced at E. Let us now check the ratio $\frac{AE}{AB}$ and $\frac{AB}{BE}$. To do so, we need to find the lengths MC and AE.

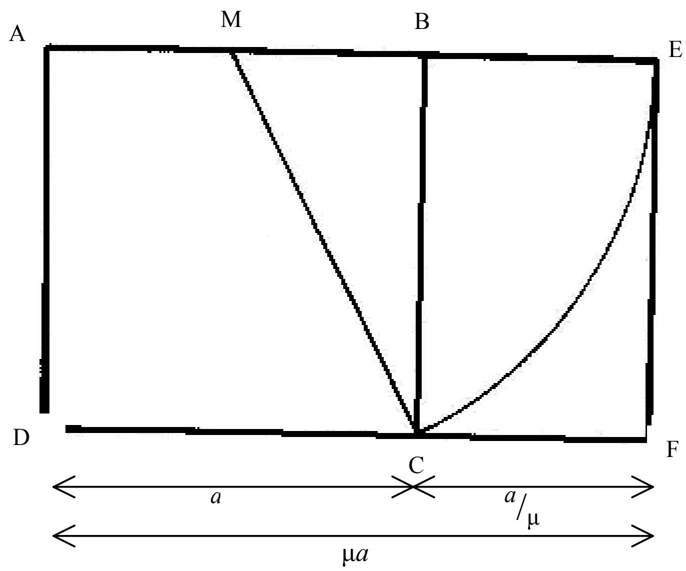

Fig 5.1.2 Extending line AB to ABE to achieve the golden ratio

By Pythagoras Theorem,
$$(MC)^2 = (MB)^2 + (BC)^2$$
$$= (a/2)^2 + a^2$$
$$= (5/4)\, a^2$$
$$MC = (\sqrt{5}/2)\, a$$

$$AE = AM + ME$$
$$= AM + MC$$
$$= (1/2)a + (\sqrt{5}/2)\, a$$
$$= 1/2\, (1 + \sqrt{5})\, a$$

$$\frac{AE}{AB} = 1/2\, (1 + \sqrt{5})$$

Now, $$\frac{AB}{BE} = \frac{a}{(\sqrt{5}/2)\, a - (1/2)a} = 1/2\, (1 + \sqrt{5})$$

So, $\frac{AE}{AB} = \frac{AB}{BE} = \mu$. Hence, we can extend any line AB to ABE by our construction to obtain the golden ratio.

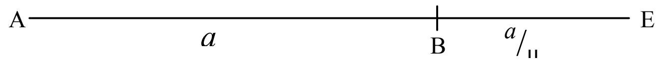

Figure 5.1.3 Extending line AB to ABE by a length of $^{a}/_{\mu}$ to achieve the golden ratio

Observe that by our construction, the rectangle AEFD has length μa and breadth a. We call rectangles with dimensions μa x a *golden rectangles*. So AEFD is a golden rectangle. From this golden rectangle, we can get lots of golden rectangles. Observe that BEFC is also a golden rectangle with dimensions EF = a and BE = $^{a}/_{\mu}$ and within this rectangle, we get another golden rectangle by removing the square of length $^{a}/_{\mu}$. Hence, we have a recursive rule of getting smaller and smaller golden rectangles from a given golden rectangle ABCD. Letting the *i*th rectangle be the rectangle obtained after the *i*th step, the recursive rule is as follows:

1) Let the *i*th rectangle $A_iB_iC_iD_i$ be of length $A_iB_i = \mu a_i$ and breadth $B_iC_i = a_i$.
2) Remove a square, with edge A_iD_i, of dimensions a_i x a_i from the rectangle.

The above construction of ABE extends AB by a length of $^{a}/_{\mu}$, such that AB is the larger part while BE is the smaller part of the new line segment. We can in fact, also extend AB to ABR, such that AB is the smaller part and BR is the larger part of the new line segment and that the ratio of BR to AB is the golden ratio. That is, if AB is of length a, then we want BR to be of length μa. By Equation (5.1), the length of BR can be expressed as $(1 + {}^{1}/_{\mu})a$. So to get BR of length μa, firstly we obtain ABE, such that BE = $^{a}/_{\mu}$. Then, using compasses centered on E with radius a, cut the line AE produced at R. Hence, we get the desired line ABR, such that $\frac{BR}{AB} = \mu$.

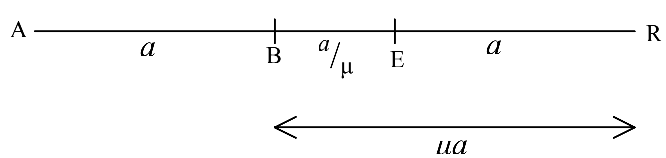

Figure 5.1.4 Extending line AB to ABR by a length of μa to achieve the golden ratio

Now, given any line AB, we can cut this line geometrically into two parts to satisfy the golden ratio. First of all, we extend AB to ABE the way we do above. Recall that if AB is of length a, then BE is of length $^{a}/_{\mu}$. Using compasses centered at B with radius BE = $^{a}/_{\mu}$, cut the line AB at X. So, BX = BE = $^{a}/_{\mu}$. Notice that AX is the smaller part while

BX is the larger part of the line segment because BX = $^{a}/_{\mu} > \frac{1}{2} a$. Since $\frac{AB}{BE} = \mu$ and BX = BE, $\frac{AB}{BX} = \frac{AB}{BE} = \mu$. Hence, any line AB can be cut geometrically into two parts to obtain the golden ratio.

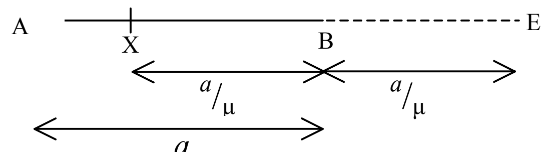

Fig 5.1.5 Cutting a given line AB into 2 parts to achieve the golden ratio

5.2 Constructing a Regular Pentagon using the Golden Ratio

We will use the golden ratio to help us construct a regular pentagon. Observe that if we divide a regular pentagon ABCDE into 5 isosceles triangles as shown in Figure 5.2.1, then, for each isosceles triangle, the interior angle at F is 72^{o}.

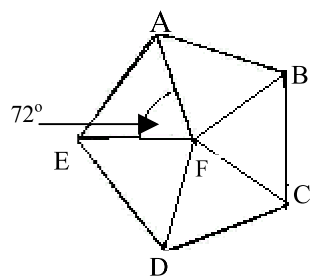

Fig 5.2.1 A regular pentagon

We will construct a regular pentagon within a circumscribing circle. To do that, we need a way to construct the angle of 72^{o}. Euclid came up with the following method to get this angle. Referring to Figure 5.2.2 is useful in understanding the following method.

1) Begin with a line ABE, which is divided into the golden ratio at B, with AB longer than BE.
2) Using compasses centered at B and E and of radius AB, draw two arcs of circles to intersect at point C. So AB = BC = CE and we will prove later that AC = AE.
3) Form the triangle CEB. Since BC = CE, so $\angle CBE = \angle CEB$. Let these two angles be α. So $\angle BCE = 180^{o} - 2\alpha$.
4) Consider the triangle ACE. Since AC = AE, $\angle ACE = \angle CEB = \alpha$. So $\angle CAB = 180° - 2\alpha$.
5) Consider the triangle ACB. $\angle ACB = \angle ACE - \angle BCE = 3\alpha. - 180°$. Since AB = BC, $\angle CAB = 3\alpha. - 180°$.
6) From (4) and (5), $\angle CAB = 3\alpha - 180° = 180° - 2\alpha$. Solving, we get $\alpha = 72°$.

Now that we obtain the angle $\alpha = 72°$ by the above construction, construct a circle at center E, radius less than BE. The circle cuts BE and CE at X and Y respectively. X and Y form two vertices of our regular pentagon. We can get the remaining three vertices of the pentagon using compasses with radius XY and cutting the circle.

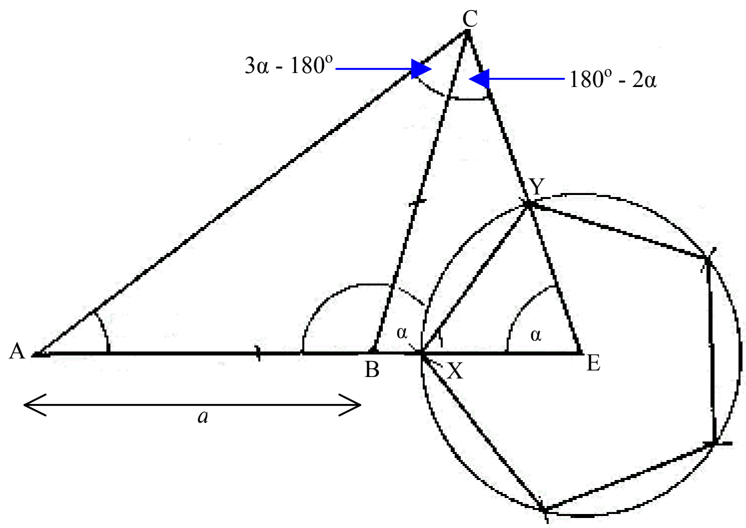

Fig 5.2.2 Constructing a regular pentagon

Now, we prove that AC = AE. Let the length of AB = a and so, BE = $^{a}/_{\mu}$. So AE = a(1 + $^{1}/_{\mu}$). By Equation (5.1), AE = μa. So we want to prove that AC = μa.

Find the mid-point N of BE and the line CN is perpendicular to BE. We apply Pythagoras Theorem to get AC.

$$
\begin{aligned}
(AC)^2 &= CN^2 + AN^2 \\
&= (CE^2 - NE^2) + (AB + BN)^2 \\
&= (a^2 - (^{a}/_{2\mu})^2) + (a + (^{a}/_{2\mu}))^2 \\
&= a^2(2 + {}^{1}/_{\mu}) \\
&= a^2 (1 + \mu) \qquad \text{by Equation (5.1)} \\
&= a^2 \mu^2 \qquad\quad\;\; \text{by Equation (5.2)}
\end{aligned}
$$

Therefore, AC = μa = AE.

5.3 The Parthenon and the Golden Ratio

Fig 5.3.1 The Parthenon

The picture on the left shows the *Parthenon*, an architecture construction by the Athenians. The Parthenon is an ancient Greek temple built to the goddess *Athena*. Many people believe that the Parthenon embodies the golden ratio in some way. They claim that the Parthenon conforms to some golden rectangles.

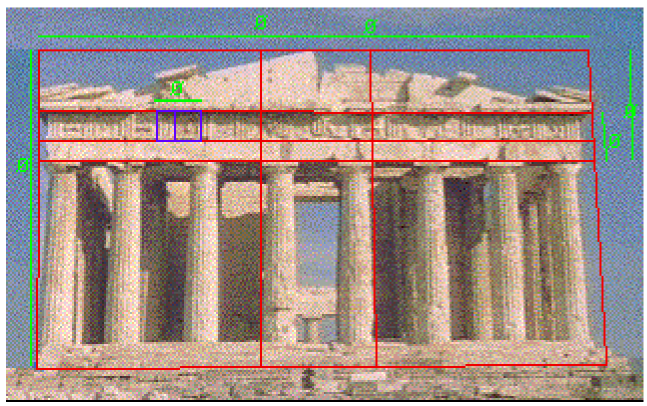

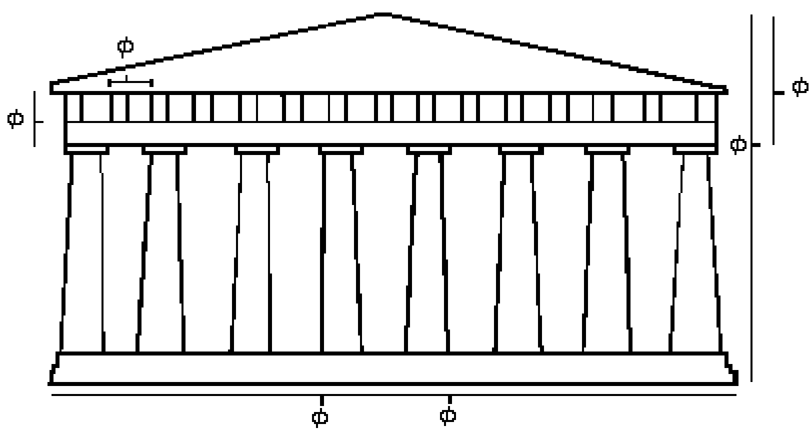

Fig 5.3.2 The Parthenon and the Golden Ratio ϕ

The above two figures are obtained from the website http://www.ee.surrey.ac.uk/Personal/R.Knott/Fibonacci/fibInArt.html. The website claims that the two figures show how the Parthenon is related to the golden ratio.

However, the website does not provide the measurements concerned to obtain the golden ratio located in the figures.

I went to the website http://cuip.uchicago.edu/~dlnarain/2001/activity2.htm and found a photograph of the front of the Parthenon. I took some measurements using the ruler on the photograph of the Parthenon presented on this website. They are as follow:

1) distance from the outmost base corner of the left pillar to the outmost base corner of the right pillar, l = 12.5cm

2) distance from the base of the pillar to the top of the pillar, d_1 = 4.1cm

3) distance from the base of the pillar to the tip of the triangular top of the Parthenon, d_2 = 6.6cm

4) distance from the base of the step closest to the pillar to the tip of the triangular top, d_3 = 6.8cm

5) distance from the base of the third step (which is also the last step) away from the pillar to the tip of the triangular top, d_4 = 7.2cm

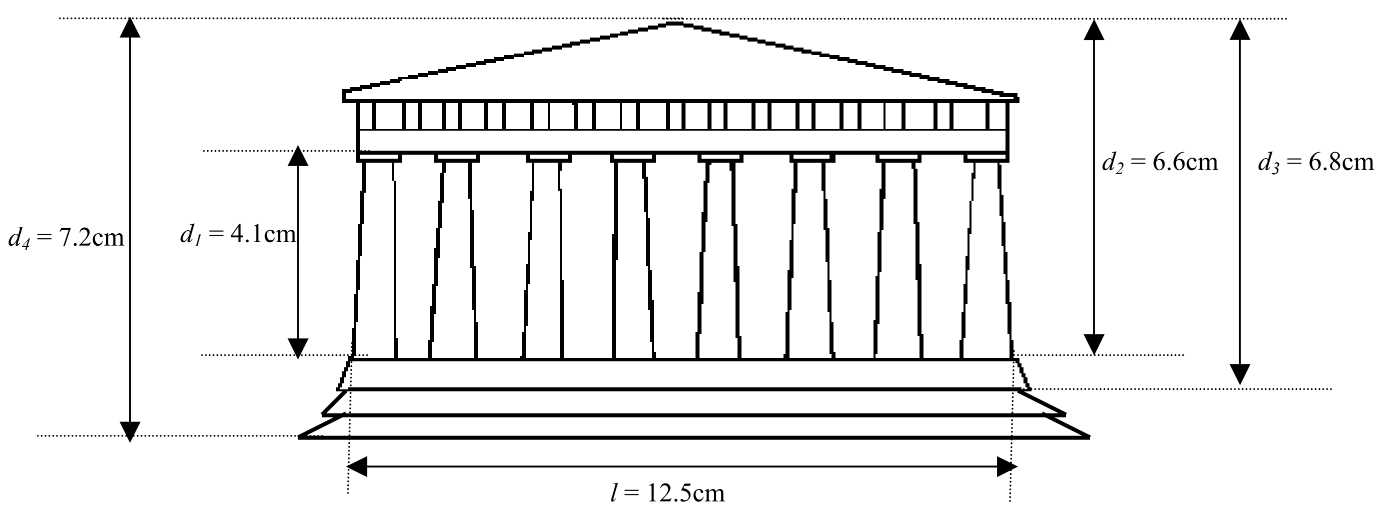

Fig 5.3.2 My measurements of the Parthenon

I computed the following ratios:

1) $^{l}/d_1 = 3.0$
2) $^{l}/d_2 = 1.9$
3) $^{l}/d_3 = 1.8$
4) $^{l}/d_4 = 1.7$

Markowsky **[26]** suggests a range of values of ratio to qualify as the golden ratio. He suggests that if the computed ratio is within 2% of the golden ratio, that is, if the computed ratio is in the range [1.58, 1.66], then there is the possibility that the golden ratio is present. He calls this range the *acceptable* range.

From my calculations, the ratio closest to the golden ratio is $^{l}/d_4 = 1.7$, which is different from the golden ratio by $\frac{1.7-1.6}{1.6}$ x 100% = 6.25%. Thus, given Markowsky's suggested range, my computed ratios cannot justify the presence of the golden ratio. However, it is essential to note my measurements might not be accurate due to hidden details of the Parthenon that arise from the smallness of the photograph and limitation to the accuracy of the ruler.

Markowsky comments that "*dimensions of the Parthenon vary from source to source probably because different authors are measuring between different points. With so many numbers available a golden ratio enthusiast could choose whatever numbers gave the best result.*" So, it can be seen that the issue of whether the Parthenon embodies the golden ratio is a controversial one.

5.4 The Golden Rectangle as the Most Aesthetically Pleasing Rectangle

Markowsky cites in his journal paper **[26]** several references that support the claim that the golden rectangle is the most aesthetically pleasing rectangle. Some of the references cited include

1) Frank Land, *The Language of Mathematics,* Doubleday, Garden City, NY, 1963
2) Margaret F. Willerding, *Mathematical Concepts*, A Historical Approach, Prindle, Weber & Schmidt, Boston, 1967
3) Leonard Zusne, *Visual Perception of Form*, Academic Press, New York, 1970

Though some of the references cited include some experiments which require their subjects to choose a most pleasing rectangle out of a variety of rectangles, Markowsky feels that the experiments have some flaws, such as, a small variety of rectangles to choose from. Furthermore, he carries out his own informal experiments using Figures 5.4.1 and 5.4.2 to find out which rectangles appeal more to people. From his experiment, he found that given both figures, people generally select different rectangles! He did another experiment with 48 rectangles with ratios ranging from 1.6 to 1.7. In this experiment, he realized that many people could not identify the golden rectangle. Thus he is not convinced that the golden rectangle is indeed the most aesthetically pleasing rectangle.

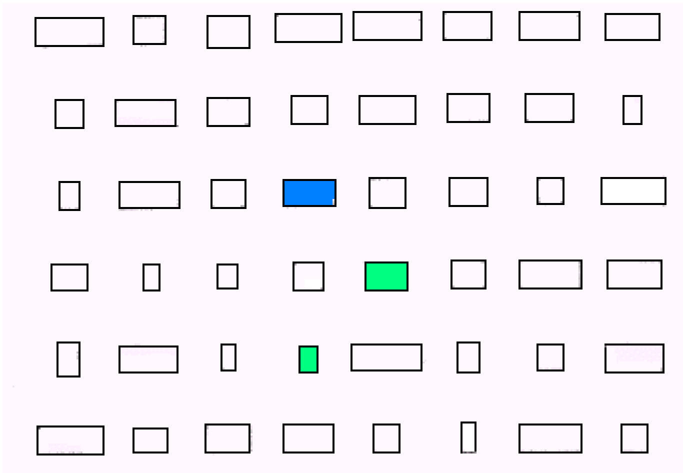

Fig 5.4.1 Rectangles with ratios ranging from 0.4 to 2.5 in random order.
Rectangles coloured in green are closest to the golden rectangle. The rectangle in blue is the one most commonly chosen by Markowsky's subjects. It has a ratio of 1.83. In the actual experiment all rectangles are not coloured.

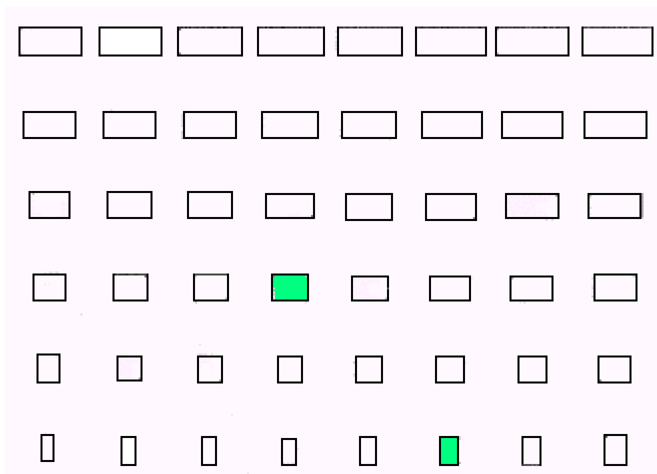

Fig 5.4.2 Rectangles with ratios ranging from 0.4 to 2.5 in linear order.
Rectangles coloured in green are closest to the golden rectangle. The actual experiment does not have the green colouring.

Inspired by Markowsky, I carried out his experiment using Figures 5.4.1 and 5.4.2, with eleven friends in my university as my subjects. I presented both figures (without any colouring) to my friends and asked them to choose a rectangle, from each figure, that looked the most pleasant or "artistic" to them. My survey form and results are tabulated in Appendix II. Only one friend chose the same rectangles in Figures 5.4.1 and 5.4.2. All the rest chose different rectangles. Generally, the rectangles chosen by all of my friends did not embody the golden ratio. Most of the rectangles they had chosen are small and some rectangles chosen are close to a square. Some friends cited "cute" as the reason for the choices they had made. Hence, my experiment shows that the golden rectangle is not necessarily the most aesthetically pleasing rectangle.

Appendix I
The Iterated Function Systems of Symmetric Fractals Presented in Table 3.6.1

The symmetric fractals presented in Chapter 3 are created using the software *Fractal Explorer* with their respective iterated function systems. In the iterated function system (*IFS*) of each of the symmetric fractals, the first affine transformation f_1 is given in Field and Golubitsky **[11]**. To get the rest of the functions in the IFS, we analyze the symmetries of each figure and compute the linear transformation matrix, t_i, of each symmetry i. Then, $f_i = t_i f_1$. Each t_i is of the form $t_i\begin{pmatrix} x \\ y \end{pmatrix} = \begin{bmatrix} a & b \\ c & d \end{bmatrix}$ and each f_i in the IFS is of the form $f_i\begin{pmatrix} x \\ y \end{pmatrix} = \begin{bmatrix} A & B \\ C & D \end{bmatrix}\begin{pmatrix} x \\ y \end{pmatrix} + \begin{pmatrix} E \\ F \end{pmatrix}$ with probability p.

If t_i corresponds to a rotation of angle θ, then $t_i = \begin{bmatrix} \cos\theta & -\sin\theta \\ \sin\theta & \cos\theta \end{bmatrix}$.

If t_i corresponds to a reflection of angle θ counter-clockwise from the positive x-axis, then $t_i = \begin{bmatrix} \cos 2\theta & \sin 2\theta \\ \sin 2\theta & -\cos 2\theta \end{bmatrix}$.

<u>The iterated function system of the Bee</u>

The Bee is of the symmetry group D_3, so it has a 3-fold rotation and 3 reflection axes. A 3-fold rotation implies that rotating the figure by $\theta_1 = 0^o$, $\theta_2 = 120^o$ and $\theta_3 = 240^o$ will leave the figure unchanged. I shall call these angles the *rotation angles*. The reflection axes are at $\theta_4 = 0^o$, $\theta_5 = 60^o$ and $\theta_6 = 120^o$ from the positive x-axis. I shall call these angles the *reflection angles*.

	Symmetry	Angle	a	b	c	d
t_1	Rotation	0^o	1	0	0	1
t_2		120^o	$-1/2$	$-\sqrt{3}/2$	$\sqrt{3}/2$	$-1/2$
t_3		240^o	$-1/2$	$\sqrt{3}/2$	$-\sqrt{3}/2$	$-1/2$
t_4	Reflection	0^o	1	0	0	-1
t_5		60^o	$-1/2$	$\sqrt{3}/2$	$\sqrt{3}/2$	$1/2$
t_6		120^o	$-1/2$	$-\sqrt{3}/2$	$-\sqrt{3}/2$	$1/2$

Using $f_i = t_i f_1$, we obtain the following functions for the IFS of the Bee.

	A	B	C	D	E	F	p
f_1	-0.10000	0.35000	0.20000	0.50000	0.50000	0.40000	0.1600
f_2	-0.12321	-0.60801	-0.18660	0.05311	-0.59641	0.23300	0.1700
f_3	0.22320	0.25801	-0.01339	-0.55311	0.09641	-0.63301	0.1700
f_4	-0.10000	0.35000	-0.20000	-0.50000	0.50000	-0.40000	0.1700
f_5	0.22321	0.25801	0.01340	0.55311	0.09641	0.63301	0.1600
f_6	-0.12320	-0.60801	0.18660	-0.05311	-0.59641	-0.23301	0.1700

<u>The iterated function system of the Doily</u>

The Doily is of the symmetry group D_8, so it has a 8-fold rotation and 8 reflection axes. Its rotation angles are $\theta_1 = 0^o$, $\theta_2 = 45^o$, $\theta_3 = 90^o$, $\theta_4 = 135^o$, $\theta_5 = 180^o$, $\theta_6 = 225^o$, $\theta_7 = 270^o$ and $\theta_8 = 315^o$. The reflection angles are at $\theta_9 = 0^o$, $\theta_{10} = 22.5^o$, $\theta_{11} = 45^o$, $\theta_{12} = 67.5^o$, $\theta_{13} = 90^o$ $\theta_{14} = 112.5^o$, $\theta_{15} = 135^o$ and $\theta_{16} = 157.5^o$.

	Symmetry	Angle	a	b	c	d
t_1	Rotation	0^o	1	0	0	1
t_2		45^o	$1/\sqrt{2}$	$-1/\sqrt{2}$	$1/\sqrt{2}$	$1/\sqrt{2}$
t_3		90^o	0	-1	1	0
t_4		135^o	$-1/\sqrt{2}$	$-1/\sqrt{2}$	$1/\sqrt{2}$	$-1/\sqrt{2}$
t_5		180^o	-1	0	0	-1
t_6		225^o	$-1/\sqrt{2}$	$1/\sqrt{2}$	$-1/\sqrt{2}$	$-1/\sqrt{2}$
t_7		270^o	0	1	-1	0
t_8		315^o	$1/\sqrt{2}$	$1/\sqrt{2}$	$-1/\sqrt{2}$	$1/\sqrt{2}$
t_9	Reflection	0^o	1	0	0	-1
t_{10}		22.5^o	$1/\sqrt{2}$	$1/\sqrt{2}$	$1/\sqrt{2}$	$-1/\sqrt{2}$
t_{11}		45^o	0	1	1	0
t_{12}		67.5^o	$-1/\sqrt{2}$	$1/\sqrt{2}$	$1/\sqrt{2}$	$1/\sqrt{2}$
t_{13}		90^o	-1	0	0	1

t_{14}		112.5^o	$-1/\sqrt{2}$	$-1/\sqrt{2}$	$-1/\sqrt{2}$	$1/\sqrt{2}$
t_{15}		135^o	0	-1	-1	0
t_{16}		157.5^o	$1/\sqrt{2}$	$-1/\sqrt{2}$	$-1/\sqrt{2}$	$-1/\sqrt{2}$

Using $f_i = t_i f_1$, we obtain the following functions for the IFS of the Doily.

	A	B	C	D	E	F	p
f_1	-0.25000	-0.30000	0.30000	-0.26000	0.50000	0.50000	0.0625
f_2	-0.38891	-0.02828	0.03535	-0.39598	0.00000	0.70711	0.0625
f_3	-0.30000	0.26000	-0.25000	-0.30000	-0.50000	0.50000	0.0625
f_4	-0.03535	0.39598	-0.38891	-0.02828	-0.70711	0.00000	0.0625
f_5	0.38891	0.02828	-0. 03536	0.39598	0.00000	-0.70711	0.0625
f_6	0.03536	-0.39598	0.38891	0.02828	0.70711	0.00000	0.0625
f_7	0.25000	0.30000	-0.30000	0.26000	-0.50000	-0.50000	0.0625
f_8	0.30000	-0.26000	0.25000	0.30000	0.50000	-0.50000	0.0625
f_9	-0.25000	-0.30000	-0.30000	0.26000	0.50000	-0.50000	0.0625
f_{10}	0.03536	-0.39598	-0.38891	-0.02828	0.70711	0.00000	0.0625
f_{11}	0.30000	-0.26000	-0.25000	-0.30000	0.50000	0.50000	0.0625
f_{12}	0.38891	0.02828	0.03536	-0.39598	0.00000	0.70711	0.0625
f_{13}	0.25000	0.30000	0.30000	-0.26000	-0.50000	0.50000	0.0625
f_{14}	-0.03536	0.39598	0.38891	0.02828	-0.70711	0.00000	0.0625
f_{15}	-0.30000	0.26000	0.25000	0.30000	-0.50000	-0.50000	0.0625
f_{16}	-0.38891	-0.02828	-0.03536	0.39598	0.00000	-0.70711	0.0625

<u>The iterated function system of the Sierpinski Polygons</u>

Though the method used in getting the IFS of the Bee and the Doily will still work for the Sierpinski polygons, here, I offer a slightly different method to get the IFS of the Sierpinski polygons. Given a Sierpinski n-gon, the smallest non-zero rotation angle is $360^o/_n$. Compute the transformation matrix t for this rotation angle. Let $f_i = A\begin{pmatrix} x \\ y \end{pmatrix} + c_i$,

$A=\begin{bmatrix} 0.5 & 0 \\ 0 & 0.5 \end{bmatrix}$. Next, given $f_1 = \begin{bmatrix} 0.5 & 0 \\ 0 & 0.5 \end{bmatrix}\begin{pmatrix} x \\ y \end{pmatrix} + \begin{pmatrix} 0.5 \\ 0 \end{pmatrix}$, we compute

$$f_{i+1} = \begin{bmatrix} 0.5 & 0 \\ 0 & 0.5 \end{bmatrix}\begin{pmatrix} x \\ y \end{pmatrix} + tc_i,\ i=1, 2, \ldots, n-1.$$

The iterated function system of the Sierpinski Triangle

	A	B	C	D	E	F	p
f_1	0.50000	0.00000	0.00000	0.50000	0.50000	0.00000	0.3000
f_2	0.50000	0.00000	0.00000	0.50000	-0.25000	0.43301	0.3000
f_3	0.50000	0.00000	0.00000	0.50000	-0.25000	-0.43301	0.4000

The iterated function system of the Sierpinski Pentagon

	A	B	C	D	E	F	p
f_1	0.50000	0.00000	0.00000	0.50000	0.50000	0.00000	0.2000
f_2	0.50000	0.00000	0.00000	0.50000	0.15450	0.47553	0.2000
f_3	0.50000	0.00000	0.00000	0.50000	-0.40451	0.29388	0.2000
f_4	0.50000	0.00000	0.00000	0.50000	-0.40450	-0.29390	0.2000
f_5	0.50000	0.00000	0.00000	0.50000	0.15451	-0.47552	0.2000

The iterated function system of the Sierpinski Hexagon

	A	B	C	D	E	F	p
f_1	0.50000	0.00000	0.00000	0.50000	0.50000	0.00000	0.1667
f_2	0.50000	0.00000	0.00000	0.50000	-0.25000	0.43301	0.1667
f_3	0.50000	0.00000	0.00000	0.50000	-0.25000	-0.43301	0.1667
f_4	0.50000	0.00000	0.00000	0.50000	0.25000	0.43300	0.1667
f_5	0.50000	0.00000	0.00000	0.50000	-0.50000	0.00000	0.1667
f_6	0.50000	0.00000	0.00000	0.50000	0.25000	-0.43300	0.1665

Appendix II
Survey on the Most Pleasant or "Artistic" Rectangle

<u>A Sample of the Survey Form</u>

Dear friends,

Please help me with this simple experiment. In each section, please place a tick in the rectangle which you think looks the most pleasant or "artistic" to you! Thanks!

Section A

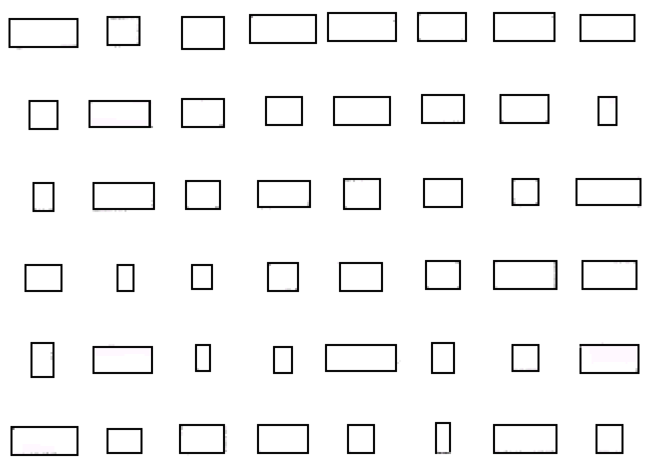

Any reason(s) for your choice?

____

____

____

____

____

Section B

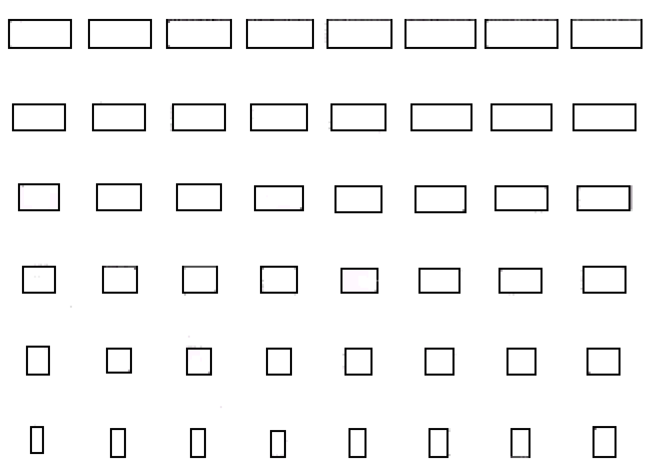

Any reason(s) for your choice?

____

____

____

____

Your Profile

Sex : ________ Age: ________ Fac/Year: ______________________________

Results of the survey

Rectangles that are chosen by only one respondent are shaded blue. Rectangles that are chosen by two respondents are shaded dark green. Rectangles that are the golden rectangles are shaded light green. Each respondent chose a rectangle in Section B that is of different proportion to that chosen in Section A.

Section A

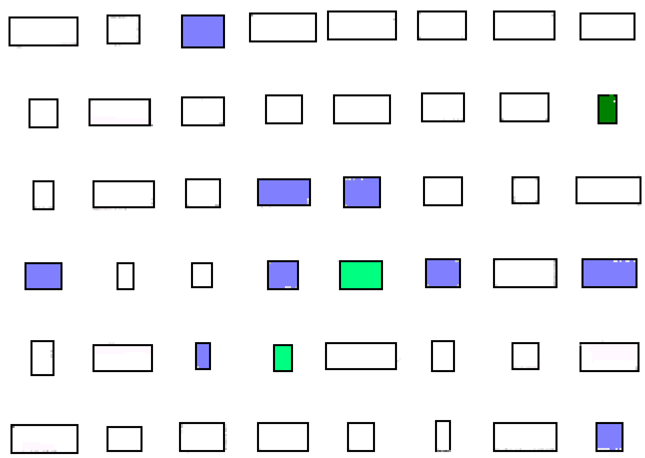

Section B

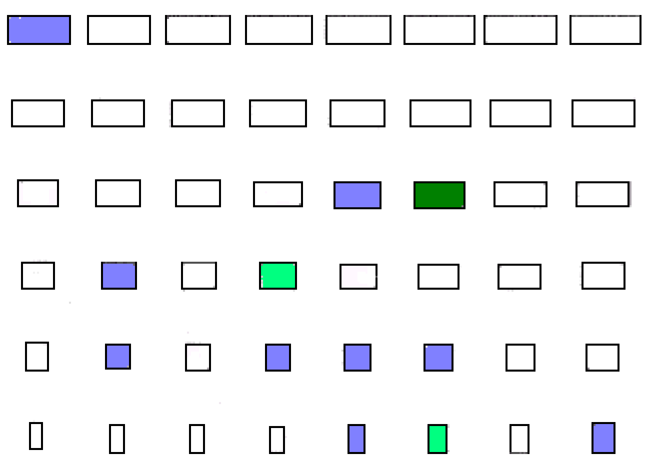

Appendix III
List of Figures Created by the Software *Kaleidomania!*™ and *Fractal Explorer*

I) List of Figures Created by *Kaleidomania!*™

II) List of Figures Created by *Fractal Explorer*

Bibliography

Chapter 1: Symmetry Groups

[1] Washburn and Crowe. *Symmetries of Culture,* University of Washington Press, 1988

[2] Schattschneider, Doris. *The Plane Symmetry Groups: Their Recognition and Notation*, American Mathematical Monthly, Vol 85, Issue 6 (Jun-Jul, 1978), 1978

[3] Kappraff, Jay. *The Geometric Bridge Between Art and Science*, McGraw –Hill, 1991

[4] http://www.xahlee.org/Wallpaper_dir/c5_17WallpaperGroups.html

[5] http://www.clarku.edu/~djoyce/wallpaper/trans.html

Chapter 2: Tilings

[6] Martin, George E. *Transformation Geometry: An introduction to Symmetry*, Springer-Verlag, 1982

[7] Grunbaum and Shephard. *Tilings and Patterns*, W.H Freeman and Company, 1987

[8]http://euch3i.chem.emory.edu/proposal/gbms01.uwgb.edu/~dutchs/symmetry/archtil.htm

Chapter 3: Fractals

[9] Tannenbaum and Arnold. *Excursions in Modern Mathematics*, 14th edition, Prentice Hall 2001

[10] Davis, Donald M. *The Nature and Power of Mathematics*, Princeton University Press, 1993

[11] Field and Golubitsky. *Symmetry in Chaos*, Oxford University Press, 1992

[12] http://www.eclectasy.com/Fractal-Explorer/index.html

[13] http://www.creativemagazine.com/fractal-explorer-help/IFS.html

[14] http://www.americanscientist.org/Issues/Sciobs96/Sciobs96-09image.html

[15] http://www.best.com/~ejad/java/fractals/koch.shtml

[16] http://www.owlnet.rice.edu/~elec539/Projects99/DRDP/proj2/

[17] http://a.die.supsi.ch/~sreffert/SIERPINSKI/APPLET.html

[18] http://www.math.vt.edu/people/hoggard/FracGeomReport/node2.html

[19] http://www.cut-the-knot.com/do_you_know/dimension.html

[20] http://abacus.bates.edu/~sross/caul.html

[21] http://www.home.aone.net.au/byzantium/ferns/fractal.html

[22] http://www.fractenna.com/nca_faq.html

Chapter 4: Kaleidoscopes

[23] Gay, David. *Geometry by Discovery*, John Wiley & Sons, Inc. 1998

[24] http://www.brewstersociety.com/mirror_config.html

Chapter 5: Golden Ratio

[25] Pedoe, Daniel. *Geometry and the Visual Arts*. Dover Publications, Inc. 1983

[26] Markowsky, George. *Misconceptions about the Golden Ratio*, The College Mathematics Journal, Vol 23, No. 1, Jan 1992

[27]http://www.richmond.edu/academics/a&s/classics/students/Cheatham/Athens.htm

[28] http://www.ee.surrey.ac.uk/Personal/R.Knott/Fibonacci/fibInArt.html

[29] http://cuip.uchicago.edu/~dlnarain/2001/activity2.htm

[30] http://www.scienceyear.com/sciteach/whoami/pdf/passport/gmpupils.pdf